BIO-INSPIRED IMMOBILIZATION OF GOLD NANOPARTICLES ONTO MAGNETIC GRAPHENE OXIDE FOR CATALYTIC REDUCTION OF NITROARENES

by

BUSHRA PARVIN UPOMA

In the partial fulfillment of the requirement for the degree

of

MASTER OF SCIENCE IN CHEMISTRY

Department of Chemistry

BANGLADESH UNIVERSITY OF ENGINEERING AND TECHNOLOGY

August 2019

Bangladesh University of Engineering and Technology
Department of Chemistry

The thesis titled "Bio-Inspired Immobilization of Gold Nanoparticles onto Magnetic Graphene oxide for catalytic Reduction of Nitroarenes'' submitted by Bushra Parvin Upoma, Roll No: 1017032706, Session: October 2017, has been accepted as satisfactory in partial fulfillment of the requirement for the degree of Master of Science in Chemistry on August 31, 2019.

BOARD OF EXAMINERS

1. Dr. Md. Shakhawat Hossain Firoz
   Professor
   Department of Chemistry
   BUET, Dhaka

   31.08.19
   Chairman

2. Dr. Md. Nazrul Islam
   Professor & Head
   Department of Chemistry
   BUET, Dhaka

   Member
   (Ex- officio)

3. Dr. Al Nakib Chowdhury
   Professor
   Department of Chemistry
   BUET, Dhaka

   Member

4. Dr. Chanchal Kumar Roy
   Assistant Professor
   Department of Chemistry
   BUET, Dhaka

   Member

5. Dr. Md. Anamul Hoque
   Professor
   Department of Chemistry
   Jahangirnagar University
   Savar, Dhaka

   Member
   (External)

CANDIDATE'S DECLARATION

It is hereby declared that this thesis or any part of it has not been submitted elsewhere for the award of any degree or diploma.

Bushra Parvin Upoma

DEDICATION

I dedicate this thesis to ….

My Beloved Parents,

Honorable Supervisor

&

Dr. Md. Shafiul Azam Sir

Table of Contents

List of Tables

List of Figures

List of Abbreviations of Technical Symbols and Terms

1. Graphene oxide (GO)
2. Magnetic Graphene oxide (MGO)
3. Polydopamine (PDA)
4. Methylene Blue (MB)
5. 4-Nitrophenol (4-NP)

Acknowledgement

At the very beginning, I humbly acknowledge my deepest gratitude to the almighty, the most gracious, benevolent and merciful creator for his infinite mercy bestowed on me in carrying out the research work presented in the dissertation.

It is a great pleasure for me to acknowledge my deepest sense of gratitude, sincere, appreciation, heartfelt indebtedness and solemn regards to my reverend teacher and supervisor Dr. Md. Shakhawat Hossain Firoz, Professor, Department of Chemistry, Bangladesh University of Engineering and Technology (BUET), for his kind supervision, indispensable guidance, valuable and constructive suggestions, liberal help and continuous encouragement during the whole period. It is obvious that his attributive contribution and efforts have greatly shaped me into what I am today. In fact, I am quite fortunate to be a part of his ambitious research team.

It is my great honor to convey my sincere gratitude to my respected teacher Professor Dr. Md. Abdur Rashid, honorable Head of the Department of Chemistry, BUET for giving me his wonderful support to move through the academic processes during this M.Sc. program. I would like to convey my deepest gratitude to Dr. Md. Shafiul Azam, Dr. Al Nakib Chowdhury, Dr. Abu Bin Imran, Dr. Chanchal Kumar Roy and Ms. Nahida Akter for their valuable suggestions, appreciated comments, guidance and help during the research period. I am thankful to all other respected teachers of the Department of Chemistry, BUET, for their time to time support. I would also like to thank all of the officers and staffs of the Department of Chemistry, BUET for their continuous help during my study period.

I am highly grateful to all members of the board of examiners for their valuable suggestions and appreciated comments.

I would like to express my sincere gratitude to Mr. A. K. M. Atique Ullah, Scientific Officer, Atomic Energy Centre, Bangladesh Atomic Energy Commission, Dhaka, Bangladesh for his generous help a nd kind support of materials characterization during the research period.

I am thankful to my dear colleagues and all the members of my Research Group for their friendly cooperation and lovely encouragement throughout my research period. Special thanks to Md. Moshfeq Uddin, Md. Ferdous and Wahidur Rahman Sajal for their continuous help during the research.

I am also thankful to other fellows of Chemistry Materials Laboratory for their cooperation during the research period.

I am grateful to the authority of BUET and The World Academy of Sciences (TWAS) for providing financial support for this research work.

Finally, I would like to express my heartfelt indebtedness and profound gratitude to my beloved father, mother and all of my family members for their continuous inspiration and immeasurable sacrifices throughout the period of my study.

August, 2019 Bushra Parvin Upoma

Abstract

There is an intense research interest on the development of a bio- inspired strategy for synthesizing magnetic graphene oxide (MGO) composite materials decorated with gold nanoparticles (AuNPs) because of their applications for the catalytic reduction of various nitroarenes. We exploited interesting dopamine chemistry to achieve in situ reduction of Au^{3+} salt to AuNPs and deposition of AuNPs on the dopamine-MGO surface. The magnetic properties were introduced in the catalyst for easy separation. Graphene oxide as supporting material has high surface area which can enhance the surface capacity by ascribing to the synergistic effect of polydopamine (PDA) with multifunctional groups. Mainly Dopamine coated on the surface of MGO in tris-buffer solution which leads to the formation of MGO-PDA composite where PDA protects AuNPs from aggregation. To compare the catalytical activity of synthesized catalyst MGO-PDA@Au, another noble metal catalyst silver was introduced and synthesized in the same steps involved in gold nanocatalyst synthesis. The resultant catalysts were characterized by employing FESEM, X-ray, EDS, TGA, FTIR and UV-Vis spectroscopy. FESEM study showed that the average size of AuNPs and AgNPs particles is 8 nm and 12 nm, respectively. Dopamine coating and the presence of o ther chemical functional groups were confirmed by FTIR spectroscopy and TGA study showed that the thermal stability of nanocomposites. To study the catalytic activity of MGO-PDA@Au, 4-nitrophenol was selected as model dye as it was UV active. Methylene blue (MB) was taken here to compare the degradation of 4-nitrophenol. In the presence of excess NaBH4, these reactions follow pseudo firstorder reaction kinetics. The reduction of organic dyes using aqueous NaBH4 is thermodynamically favorable, but kinetically not feasible due to the large potential difference between donor and acceptor molecules. The metal NPs accelerates the reaction by facilitating electron relay from the donor $BH4^-$ to acceptor dye molecules thereby overcome the kinetic barrier. After the reaction of catalysis for MGO-PDA@Au catalysts degrade 4-NP and MB almost 96.4% in 7min and 98.9% in 5min respectively. So, MGO-PDA@Au composite materials exhibited good synergistic capabilities of efficient catalytic reduction efficiency along with fast red uction kinetics as tested for both dyes.

CHAPTER 1

Introduction

Nitroarenes are the largest and most important groups in industrial chemicals. These compounds are organic molecules that consist of at least one nitro group (-NO2) attached to an aromatic ring. The vast majority are synthetic, although several biologically produced nitroaromatic compounds have been identified. The strong electronegativity of the nitro group stems from the combined action of the two electron-deficient oxygen atoms bonded to the partially positive nitrogen atom. When attached to a benzene ring, the nitro group is able to delocalize π-electrons of the ring to satisfy its own charge deficiency. This not only provides charge to the molecule but also imparts unique properties that make the nitro group an important functional group in chemical syntheses. The nitro group is strongly deactivating toward electrophilic aromatic substitution of the benzene ring. Both the conjugation state and resonance properties of nitro groups attached to aromatic rings result in partially positive charges at ortho and para positions that act to repel electrophiles, and as a consequence, attacks are directed toward the open meta positions [1].

Nitroaromatic compounds are released into the biosphere almost exclusively from anthropogenic sources. Some compounds are produced by incomplete combustion of fossil fuels; others are used as synthetic intermediates, dyes, pesticides, and explosives. Recent research revealed a number of microbial systems capable of transforming or biodegrading nitroaromatic compounds. Anaerobic bacteria can reduce the nitro group via nitroso and hydroxylamine intermediates to the corresponding amines.

The toxicity of nitroarenes and their metabolites has been studied in a variety of systems [2, 3]. Both the nitro group and the amino group are relatively stable in biological s ystems. The interconversion between nitro and amino group, however, involves the intermediate production of the corresponding nitroso and hydroxylamine derivatives which are very reactive and, in many instances, more toxic than the parent molecules give so me more adverse effect of nitroarenes

Therefore, suitable methods for the treatment of these toxic compounds are necessary. The chemical reduction of the aromatic nitro compounds to their amino analogues is one of the effective method for the removal of such compounds from contaminated water [4, 5] This method is advantageous over other techniques such as adsorption [6, 7], degradation [8, 9],

electrochemical methods [10], coagulation/flocculation [11, 12], filtration [13, 14] etc. due to its ability to convert such toxic compounds to useful amino products.

One of the most commonly known methods is the filtration technology. Filtration methods such as ultrafiltration, nanofiltration and reverse osmosis have been used for water reuse and chemical recovery [15, 16]. In the textile industry, these filtration methods c an be used for both filtering and recycling of not only pigment rich wastewaters, but also mercerizing and bleaching wastewaters. The specific temperature and chemical composition of the wastewaters determines the type and porosity of the filter be applied. Further, the utilization of membrane technology for dye removal from textile wastewater is very effective as reported by various researchers [17][18]. However, the main drawbacks of membrane technology are the high cost, freque nt membrane fouling, the requirement of different pretreatments depending upon the type of influent wastewaters, and production of concentrated dye-bath which further needs proper treatment before its safe disposal to the environment [19, 20]. For membrane filtration, proper pretreatment units for removing suspended solid of the wastewaters are almost mandatory to increase the life time of the membranes. These make the process more expensive and thereby limit the application. Chemical coagulation and flocculation in wastewater treatment involve the addition of chemicals to alter the physical state of dissolved and suspended solids and facilitate their removal by sedimentation. Coagulation of dye-containing wastewater has been used for many years as main treatment or pretreatment due to its low capital cost [21, 22].

However, the majorlimitation of this process is the generation of sludge and ineffective decolorization of some soluble dyes [21, 23].

Adsorption method for color removal is based on the affinity of various dyes for adsorbents. It is influenced by physical and chemical factors such as dye adsorbent interactions, surface area of adsorbent, particle size, temperature, pH and contact time [19, 24]. Activated carbon is the most commonly used adsorbent and can be very effective for many dyes [25]. However, efficiency is directly dependent upon the type of carbon material used and wastewater characteristics [19]. The limitations of this technology are the eco-friendly disposal of spent adsorbents, excessive maintenance costs, and pretreatment of wastewater to reduce the suspended solid.

Synthetic dyes are found in a wide range of products such as clothes, leather accessories, and furniture. These dyes are commonly used every day. However, a side effect of their widespread use is that up to 12% of these dyes are wasted during the dying process and about 20% of this wastage enters the environment (mainly into water supply) [26]. Dye degradation is a process in which the large dye molecules are broken down chemically into smaller molecules. The resulting

products are water, carbon dioxide, and mineral byproducts that give the original dye its color. During the dyeing process, not all of the dye molecules are used. The water waste that the industry releases contain a percentage of these dye molecules. Dye molecules persist in the environment because many of them are not reactive towards light, acids, bases and oxygen. The color of the material becomes permanent. Heterogeneous photocatalysis is a widely accepted technique of choice for environmental purification [27]. The standard experimental set up for dye degradation photocatalysis is by using a UV lamp to provide energy for the creation of oxidizing radicals. Photocatalysis is the addition of light to a semiconductor oxide/sulphide that results in electrons moving from the valence band to the conduction band. The electron-hole pairs formed will react with oxygen and water molecules to create superoxide anions and hydroxide radicals that have increased oxidizing and reducing abilities to be used on numerous industrial dye compounds.

Many dyes, specifically in the textile industry such as methylene blue or methyl red, are released into ecosystems through water waste [28]. Many of these dyes can be carcinogenic and can come into contact with humans. As a result, newer treatments of the water waste are still in development.

Modification on catalysts structure and use of noble metal nanoclusters on organic or inorganic supports constitute one of the main applications widely exploited. The value of nanoparticles (NPs) is one of the most important discoveries that have recently been developed in catalysis. Metal nanoclusters, as building blocks for preparing heterogeneous catalysts, offer new possibilities of universal significance for designing and constructing structure controllable catalysts [29-31]. Noble metal nanoparticles have attracted huge attention owing to their excellent catalytic properties and their potential applications to remove the organic dyes and hazardous chemicals [32, 33]. For example, Au, Pd, Cu, Ni, Fe, and Pt nanoparticles among them gold nanoparticles (AuNPs) exhibit better interaction with visible light than any other known organic or inorganic chromophore because of its greater density of conducting electrons. The high surface energy of the nanoparticles usually causes AuNPs to aggregate extensively and therefore require stabilizers and supporting materials to generate homogenously distributed samples. Synthesizing supporting material with multi functionality ensuring the high catalytic

efficacy is therefore a great challenge for the researchers. Among these methods, catalytic degradation has received much attention because of the high efficiency, simplicity and economy [34] [35-37]. Therefore, there is a demand for an efficient heterogeneous catalyst which canreduce the aromatic nitro compounds to the corresponding amino derivatives. Catalytic reduction of nitroarene is a key reaction for two important reasons: First of all because it is one of the most utilized remediation applications for the removal of nitro compo unds from the environment and secondly because hydrogenation of nitro aromatics is considered as the most effective way to produce corresponding amino aromatics and has been widely used in production scale. Explain why you have designed Au nanoparticles on Magnetic GO.

In this study, graphene oxides were prepared by modified Hummers method [38]. To attain magnetic behavior, Fe_3O_4 was incorporated in GO by modified co-precipitation method [39]. A thin layer of dopamine was coated onto magnetic graphene oxide (MGO) by self-polymerization. After that gold nanoparticles are loaded onto polydopamine layer by in situ reduction and forming the desired catalyst MGO-PDA@Au. For the comparison silver nanocatalyst (MGO-PDA@Ag) was synthesized with the same procedure. The phase identification and crystallinity of the sample were analyzed using X-ray diffraction (XRD) technique from which the crystallite size, interlayer spacing and lattice parameters of the nanocatalyst were estimated. The chemical structural features of the prepared nanomaterials were confirmed by Fourier Transform Infrared (FT-IR) spectroscopic technique. The surface morphology was monitored by Scanning Electron Microscopy (SEM). The elemental analyses of the materials were estimated using Energy Dispersive X-ray (EDX) method. Thermogravimetric analyses were used to show the thermal stability and the proper phase transitional behavior of the desired nanomaterials as well as the relation between the phase, particle size and temperature. The catalytic properties of the prepared materials were examined by UV-VIS spectrometer. Two dyes 4-nitrophenol and Methylene blue were selected to observe the catalytical process by catalyst on UV. At first, the reaction was conducted only with dyes and NaBH4 where no catalyst was added. The reaction procedure was observed by UV spectrum. Again, the reaction between dyes and NaBH4 was conducted by adding synthesized MGO-PDA@Au catalyst and

observed until the reaction was completed and the percentage of reduction was calculated. After that, the observation proceeded with another catalyst MGO-PDA@Ag. The catalytical reduction of both catalysts was compared.

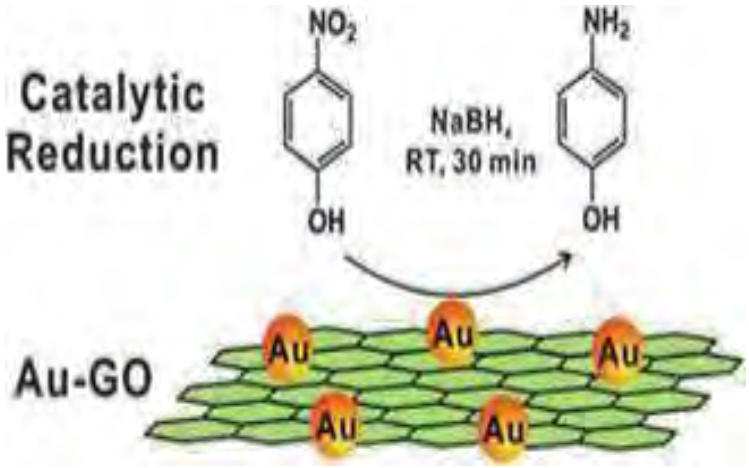

Figure 1.1 Catalytic reductions of Nitroarenes by gold NPs.

The main objective of the research is to synthesize graphene oxide (GO) and dopamine based magnetic nanocatalyst containing AuNPs. GO provide a high surface area that was synthesized by the modified Hummer's method and ferrous a nd ferric chloride was used to incorporate magnetic property. Afterward polydopamine was coated using Tris-HCl (pH8.5) buffer. Finally, gold nanoparticles were loaded on the polydopamine layer by in situ reduction of Au^{3+} to Au followed by immobilization of as- formed Au NPs onto the polydopamine coated magnetic GO. This as-prepared catalyst is characterized by employing some state-of-the-art techniques such as scanning electron microscope (SEM), X-ray diffraction (XRD), thermal analysis, magnetization

property and other common techniques like FTIR and UV-Vis spectroscopy. This nanocomposite may be used for investigation of the catalytic performance for the catalytical reduction of nitroarenes. Again, AgNPs were synthesized with same steps to analyze and se t comparison between two noble metals (Au and Ag) for catalytic reduction performance. Last of all having magnetic iron nanoparticles enables to separate nanocatalyst easily by magnet from solution.

References

[1] K.-S. Ju and R. E. Parales, "Nitroaromatic compounds, from synthesis to biodegradation," *Microbiology and molecular biology reviews: MMBR,* vol. 74, pp. 250-272, (2010).

[2] C. E. Cerniglia and C. C. Somerville, "Reductive Metabolism of Nitroaromatic and Nitropolycyclic Aromatic Hydrocarbons," in *Biodegradation of Nitroaromatic Compounds*, J. C. Spain, Ed., ed Boston, MA: Springer US, pp. 99-115, (1995).

[3] P. P. Fu, "Metabolism of Nitro-Polycyclic Aromatic Hydrocarbons," *Drug MetabolismReviews,* vol. 22, pp. 209-268, (1990).

[4] J. Huang, S. Vongehr, S. Tang, H. Lu, and X. Meng, "Highly Catalytic Pd−Ag Bimetallic Dendrites," *The Journal of Physical Chemistry C,* vol. 114, pp. 15005-15010, (2010).

[5] C.-Y. Chiu, P.-J. Chung, K.-U. Lao, C.-W. Liao, and M. H. Huang, "Facet-Dependent Catalytic Activity of Gold Nanocubes, Octahedra, and Rhombic Dodecahedra toward 4 - Nitroaniline Reduction," *The Journal of Physical Chemistry C,* vol. 116, pp. 23757-23763, (2012).

[6] I. Ivančev-Tumbas, R. Hobby, B. Küchle, S. Panglisch, and R. Gimbel, "p-Nitrophenol removal by combination of powdered activated carbon adsorption and ultrafiltration – Comparison of different operational modes," *Water Research,* vol. 42, pp. 4117-4124, (2008).

[7] A. Mehrizad, K. Zare, H. Aghaie, and S. Dastmalchi, "Removal of 4-chloro-2-nitrophenol occurring in drug and pesticide waste by adsorption onto nano-titanium dioxide," *International Journal of Environmental Science and Technology,* vol. 9, pp. 355-360, (2012).

[8] A. George, D. Selvan, and S. Mandal, *Catalytic Reduction of Toxic Nitroarenes inAqueous Medium Using Worm-Like Rhodium Nanoparticles* vol. 2, (2017).

[9] P. Xiong, Y. Fu, L. Wang, and X. Wang, "Multi- walled carbon nanotubes supported nickel ferrite: A magnetically recyclable photocatalyst with high photocatalytic activity on degradation of phenols," *Chemical Engineering Journal,* vol. 195-196, pp. 149-157, (2012).

[10] P. Jiang, J. Zhou, A. Zhang, and Y. Zhong, "Electrochemical degradation of p-nitrophenol with different processes," *Journal of Environmental Sciences,* vol. 22, pp. 500-506, (2010).

[11] B. Shi, G. Li, D. Wang, C. Feng, and H. Tang, "Removal of direct dyes by coagulation: The performance of preformed polymeric aluminum species," *Journal of Hazardous Materials,*
vol. 143, pp. 567-574, (2007).

[12] E. Guibal and J. Roussy, "Coagulation and flocculation of dye-containing solutions using a biopolymer (Chitosan)," *Reactive and Functional Polymers,* vol. 67, pp. 33-42, (2007).

[13] M. K. Purkait, S. DasGupta, and S. De, "Removal of dye from wastewater using micellar-enhanced ultrafiltration and recovery of surfactant," *Separation and Purification Technology,*
vol. 37, pp. 81-92, (2004).

[14] N. Zaghbani, A. Hafiane, and M. Dhahbi, "Separation of methylene blue from aqueous solution by micellar enhanced ultrafiltration," *Separation and Purification Technology,* vol. 55, pp. 117-124, (2007).

[15] M. Marcucci, G. Nosenzo, G. Capannelli, I. Ciabatti, D. Corrieri, and G. Ciardelli, "Treatment and reuse of textile effluents based on new ultrafiltration and other membrane technologies," *Desalination,* vol. 138, pp. 75-82, (2001).

[16] C. Fersi and M. Dhahbi, "Treatment of textile plant effluent by ultrafiltration and/or nanofiltration for water reuse," *Desalination,* vol. 222, pp. 263-271, (2008).

[17] S. Ledakowicz, M. Solecka, and R. Zylla, "Biodegradation, decolourisation and detoxification of textile wastewater enhanced by advanced oxidation processes," *Journal ofBiotechnology,* vol. 89, pp. 175-184, (2001).

[18] A. L. Ahmad, W. Azlina Harris, S. Syafiie, and O. Seng, *Removal of Dye FromWastewater of Textile Industry Using Membrane Technology* vol. 36, (2002).

[19] T. Robinson, G. McMullan, R. Marchant, and P. Nigam, "Remediation of dyes in textile effluent: a critical review on current treatment technologies with a proposed alternative,"

[20] A. Akbari, S. Desclaux, J. C. Rouch, P. Aptel, and J. C. Remigy, "New UV-photografted nanofiltration membranes for the treatment of colored textile dye effluents," *Journal ofMembrane Science,* vol. 286, pp. 342-350, (2006).

[21] Y. Anjaneyulu, N. Sreedhara Chary, and D. Samuel Suman Raj, "Decolourization of Industrial Effluents – Available Methods and Emerging Technologies – A Review," *Reviews inEnvironmental Science and Bio/Technology,* vol. 4, pp. 245-273, (2005).

[22] V. Golob, A.Vinder, and M. Simonič, "Efficiency of the coagulation/flocculation

method for the treatment of dyebath effluents," *Dyes and Pigments,* vol. 67, pp. 93-97, (2005).

[23] F. I. Hai, K. Yamamoto, and K. Fukushi, "Hybrid Treatment Systems for Dye Wastewater," *Critical Reviews in Environmental Science and Technology,* vol. 37, pp. 315-377, (2007).

[24] H. Patel and R. T. Vashi, "Treatment of Textile Wastewaterby Adsorption andCoagulation," *E-Journal of Chemistry,* vol. 7, pp. 1468-1476, (2010).

[25] G. M. Walker and L. R. Weatherley, "Adsorption of acid dyes on to granular activated carbon in fixed beds," *Water Research,* vol. 31, pp. 2093-2101, (1997).

[26] M. A. Rauf and S. S. Ashraf, "Fundamental principles and application of heterogeneous photocatalytic degradation of dyes in solution," *Chemical Engineering Journal,* vol. 151, pp. 10-18, (2009).

[27] V. U. Pandit, S. S. Arbuj, Y. B. Pandit, S. D. Naik, S. B. Rane, U. P. Mulik*, et al.*, "Solar light driven dye degradation using novel organo–inorganic (6,13-pentacenequinone/TiO2) nanocomposite," *RSC Advances,* vol. 5, pp. 10326-10331, (2015).

[28] C. P. Huang, Y. F. Huang, H. P. Cheng, and Y. H. Huang, "Kinetic study of an immobilized iron oxide for catalytic degradation of azo dye reactive black B with catalytic decomposition of hydrogen peroxide," *Catalysis Communications,* vol. 10, pp. 561-566, (2009).

[29] Z. Kónya, V. F. Puntes, I. Kiricsi, J. Zhu, P. Alivisatos, and G. A. Somorjai, "Novel Two-Step Synthesis of Controlled Size and Shape Platinum Nanoparticles Encapsulated in Mesoporous Silica," *Catalysis Letters,* vol. 81, pp. 137-140, (2002).

[30] J. Zhu, Z. Kónya, V. F. Puntes, I. Kiricsi, C. X. Miao, J. W. Ager*, et al.*, "Encapsulation of Metal (Au, Ag, Pt) Nanoparticles into the Mesoporous SBA-15 Structure," *Langmuir,* vol. 19, pp. 4396-4401, (2003).

[31] T. Yonezawa, H. Matsune, and N. Kimizuka, "Formation of an Isolated Spherical Three-Dimensional Nanoparticle Assembly as Stable Submicrometer-Sized Units by Using an Inorganic Wrapping Technique," *Advanced Materials,* vol. 15, pp. 499-503, (2003).

[32] L. Ai and J. Jiang, "Catalytic reduction of 4-nitrophenol by silver nanoparticles stabilized on environmentally benign macroscopic biopolymer hydrogel," *Bioresource Technology,* vol. 132, pp. 374-377, (2013).

[33] B. Subash, B. Krishnakumar, M. Swaminathan, and M. Shanthi, "Highly Efficient, Solar Active, and Reusable Photocatalyst: Zr-Loaded Ag–ZnO for Reactive Red 120 Dye

Degradation with Synergistic Effect and Dye-Sensitized Mechanism," *Langmuir,* vol. 29, pp. 939-949, (2013).

[34] X. Zhuang, Y. Wan, C. Feng, Y. Shen, and D. Zhao, "Highly Efficient Adsorption of Bulky Dye Molecules in Wastewater on Ordered Mesoporous Carbons," *Chemistry ofMaterials,* vol. 21, pp. 706-716, (2009).

[35] M. Iram, C. Guo, Y. Guan, A. Ishfaq, and H. Liu, "Adsorption and magnetic removal of neutral red dye from aqueous solution using Fe3O4 hollow nanospheres," *Journal of HazardousMaterials,* vol. 181, pp. 1039-1050, (2010).

[36] T. Sun, Z. Zhang, J. Xiao, C. Chen, F. Xiao, S. Wang, *et al.*, "Facile and Green Synthesis of Palladium Nanoparticles-Graphene-Carbon Nanotube Material with High Catalytic Activity," *Scientific Reports,* vol. 3, p. 2527, (2013).

[37] M. Zhang, P. Xia, L. Wang, J. Zheng, Y. Wang, J. Xu, *et al.*, "Synthesis and fabrication of CNTs/Fe3O4@Pdop@Au nanocables by a facile approach," *RSC Advances,* vol. 4, pp. 44423-44426, (2014).

[38] H. Tetsuka, R. Asahi, A. Nagoya, K. Okamoto, I. Tajima, R. Ohta, *et al.*, "Optically Tunable Amino-Functionalized Graphene Quantum Dots," *Advanced Materials,* vol. 24, pp. 5333-5338, (2012).

[39] J. Zhang, M. S. Azam, C. Shi, J. Huang, B. Yan, Q. Liu, *et al.*, "Poly(acrylic acid) functionalized magnetic graphene oxide nanocomposite for removal of methylene blue," *RSCAdvances,* vol. 5, pp. 32272-32282, (2015).

Chapter 2
Background

2.1 Background

Catalysis is the driving force behind the development of the chemical industry, which can not only make us use natural resources more efficiently, but also reduce the pollution in the processes of the chemical industry. In the last century, catalysis has b ecome the foundation of the large-scale production of the chemical and petroleum industry [1-4]. However, there still exist some problems to be solved [5, 6]. With the development of nanotechnology, catalysis has ushered in some new challenges and opportunities.

In recent years, certain achievements have been made in the metal nanomaterials as heterogeneous catalysts [7-10]. These catalysts have a very high catalytic activity and selectivity for specific reactions. Nanocatalysts for catalytic chemical reactions mainly include the oxidation reaction, the reduction reaction, coupling reaction and the electrochemical reaction [11].Noble metal nanocatalysts have attracted huge attention owing to their excellent catalytic properties and their potential applications to remove the organic dyes and hazardous chemicals [12, 13]. Nobel metals like Au [14], Pd [15], Ag [16] and Pt [17] are more popular. Among them AuNPs based nanocatalysts have shown highly active catalytic properties in many reactions, such as selective hydrogenation of organic molecules, carbon monoxide (CO) oxidation, and the water-gas shift reaction [18].

One of the universal concerns is related to the pollution of water resources by the organic dyes released from textile and fiber dyeing industries. These compounds are hazardous for human health, animals, plants and the environment. Consequently, they should be removed from water and wastewater to protect living species and the environment [19]. A well-known example of toxic dyes is 4-nitrophenol (4-NP), which affects the kidneys, liver and central nervous system of animals and humans and leads to many diseases [20]. This organic dye cannot be easily converted into non-hazardous products due to its low water solubility and high chemical stability. However, some chemical routes can help to reduce it to 4 -aminophenol (4-AP), which can inhibit corrosion and act as a substrate for synthesis of antipyretic and analgesic agents [21].Therefore, the reaction of 4-NP reduction to 4-AP is an important chemical conversion process from both industrial and environmental perspectives. To prompt this reaction, transfer of electron from the$NaBH_4$ donor to the 4-NP acceptor can be facilitated by the means of an

appropriate catalyst, such as metal nanoparticles (NPs) [22]. Catalytic reduction of nitroarenes is a key reaction for two important reasons: First of all because it is one of the most utilized remediation applications for the removal of nitro compounds from the environment and secondly because hydrogenation of nitro aromatics is considered as the most effective way to produce corresponding amino aromatics and has been widely used in production scale. It is well-known that nitro compounds are important contaminants for the environment and living organisms as well [23, 24]. Their toxic and carcinogenic nature due to the presence of nitro groups in their structure is widely demonstrated. Several remediation methods are proposed in literature such as photocatalytic degradation [25]or electrochemical methods [26].Nevertheless, the reduction of nitro groups into amino compounds through catalytic hydrogenation is one of the most utilized [27].Significant progress has been achieved in the field of nitro aromatic compounds reduction under catalysis by supported gold nanoparticles (Au NPs).The catalytic activity of AuNPs is strongly dependent on their sur face chemistry. The high surface energy of the nanoparticles usually causes AuNPs to aggregate extensively and therefore require stabilizers and supporting materials to generate homogenously distributed samples [28, 29]. Synthesizing supporting material with multi functionality ensuring the high catalytic efficacy is therefore a great challenge for the researchers.

2.2 Catalyst

A catalyst is a substance that increases the rate of a reaction, without being used up itself. Remember that if it got used up, then it would be a reactant. This process is called 'catalysis'. By using catalytic reagent, one can reduce the temperature of a chemical transformation, reduce reagent-based waste and increase the selectivity of a reaction that avoids the unwanted side reactions which leads to the green chemistry. Catalysts are the silent heroes of the chemical reactions that make human society tick. A catalyst would be that substance that would give you an option of a shortcut, bypassing that le ngthy, snaking road. By giving you a new alternate route, you can proceed to go towards saving time and energy. Biocatalysts are called Enzymes.

2.3 How Do Catalysts Work

The simplest way to understand how a catalyst works is that they lower the activation energy required to initiate a chemical reaction. Activation energy is the energy barrier that must be

surmounted in order to begin a chemical reaction. By lowering the activation energy barrier, it shows a 'new' path for the reaction to occur. If you are familiar with energy profile diagrams, you can see the difference between catalyzed and un-catalyzed reactions.

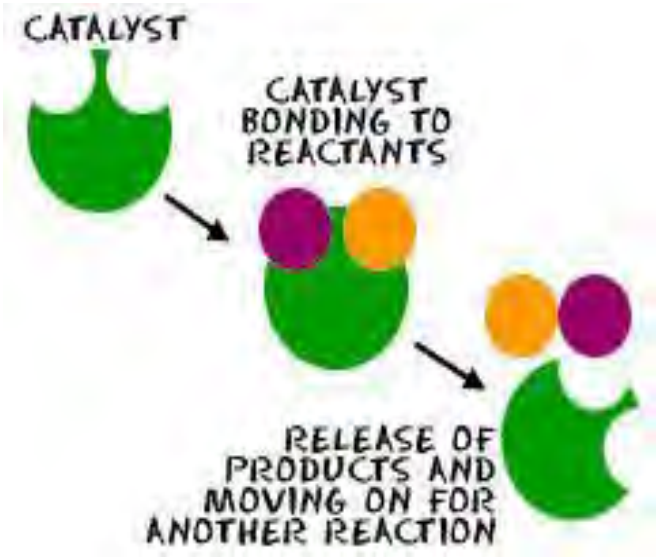

Figure 2.1 Working mechanism of a catalyst

2.4 Importance of catalyst

Catalyst increases the rate of reaction, lowers the activation energy barrier and improves the yield. It saves time and energy to get the same results in the end. The modern industrialized world would be inconceivable without catalysts. There is no other technical principle that combines economic and ecological values as closely as catalysis. The development of chemical products in advanced, industrialized societies will only be technically, economically, and ecologically by means of specific catalysts. Examples inc lude the specific production of stereo-chemically pure pharmaceuticals, the construction of tailored polymer materials, the reduction of pollutants from manufacturing plants and combustion systems (e.g. , power stations, motor vehicles). Another major topic for the twenty-first century, the production, storage, and conversion of energy, will also be promoted by catalysts. Thus, catalysis is the No. 1 technology in chemical industry: 95% of all products (volume) are synthesized by means of catalysis; 70% of all products (processes) are synthesized by means of catalysis; 80% of the added value in chemical industry is based on catalysis. Approximately 80% of all catalytic processes require heterogeneous catalysts, 15% homogeneous catalysts, and 5% biocatalysts. The total commercial value of all catalysts worldwide is over US$ 17.2 billion in 2014. In crude oil refining processes, the catalysts costs amount to only about 0.1% of the product value, and for petrochemicals this value is about 13

0.22%. Estimates suggest that catalysis contributes to >35% of the world's GDP (gross domestic product).

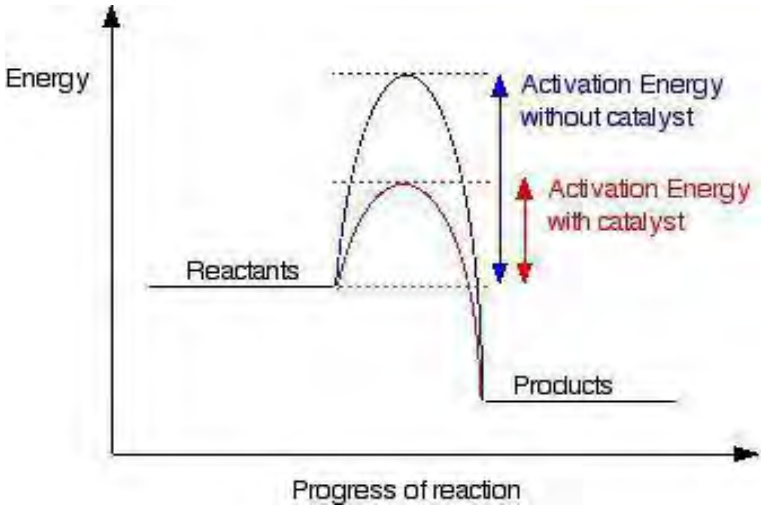

Figure 2.2 Energy profile diagram

2.5 Types of Catalyst

Catalysts are classified into several types, such as heterogeneous catalysts, homogeneous catalysts, photocatalysts, enzymes and biocatalysts and nanocatalysts.

2.5.1 Homogeneous Catalyst

This type of catalyst is in the same phase as reactant but the mechanistic principle can be invoked in heterogeneous catalysts. Usually homogeneous catalysts are dissolved in solvent with substrate. One example of homogeneous catalysis is the effect of H+ on the esterification reaction of carboxylic acids, such as the formation of methyl acetate from acetic acid and methanol [30].

2.5.2 Heterogeneous Catalyst

Heterogeneous catalysts are a substance that acts in a different phase than reactants. Most heterogeneous catalysts are solids that act on substrates in a liquid or gaseous reaction matrix. Heterogeneous catalyst has active side, which is atom or crystal faces where the reaction actually occurs. For example, in the Haber process finely divided iron particles act as a catalyst to synthesize ammonia gas from nitrogen and oxygen. The reacting gases absorb onto the reactive side onto iron particles and the resultant is ammonia gas [31].

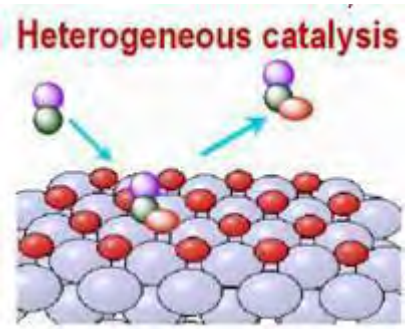

Figure 2.3 Photocatalyst

Generally speaking, photocatalysis is one kind of reaction that usages light to activate a substance that modifies the rate of a chemical reaction without being involved itself. On the other hand, photocatalyst is the substance that modifies the rate of chemical reaction using light irradiation. For example, chlorophyll is a typical natural photocatalyst where TiO_2 is man-made photocatalyst. Chlorophyll photocata lyst usually captures sunlight to turn carbon dioxide and water into oxygen and glucose (here bellow mentioned as photocatalyst), but on the contrary TiO_2 photocatalyst creates strong oxidation agent and electronic holes to breakdown the organic matter to carbon dioxide and water in the presence of photocatalyst, light and water [32].

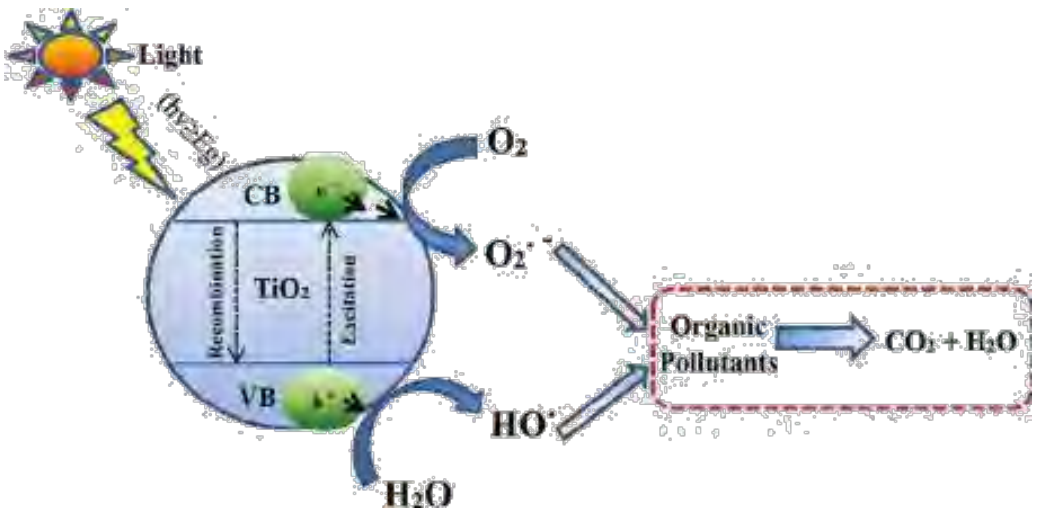

Figure 2.4 Schematic illustration of photo catalytic technique

2.5.3 Electro catalyst

Electro catalyst catalyst acts in the modification of electrochemical reactions occurring on an electrode surface. Electro catalysts are a specific form of catalyst that functions at electrode surfaces or may be the electrode surface itself. In fuel cells, different metal-containing catalysts are used to increase the rate of the half-reactions. Ruthenium (IV) oxide is widely used as an electro catalyst for producing chlorine, chlorine oxides [33].

2.5.4 Enzymes and biocatalyst

Biocatalyst is a substance that initiates or modifies a chemical reaction in a living body is termed as biocatalyst. Enzymes are known as protein-based catalysts in biology in the field of metabolism and catabolism. Most of the biocatalysts are enzymes, but other non-protein-based molecules also exhibit catalytic properties including ribozymes, and synthetic deoxy ribozymes [34].

2.6 Nanocatalyst

The field of nanocatalysis is not as new as could be expected from the current nano hype. Actually, its concept is known since the 1950s when the term nanotechnology was not even known. However, nanocatalysis is a process in which catalysis procedure use nanotechnology, so nanocatalyst is a catalyst composed of nanoparticles smaller than 100 nm in at least one-dimension porous compounds having pour diameters not bigger than 100 nm. Nanocatalysts have simultaneous advantages of both homogeneous and heterogeneous catalytic systems. Nan catalytic system allows rapid, selective chemical transformations with excellent product yield coupled with the ease catalyst separation and recovery. Recover y of catalyst from the system is a more important characteristic of any catalyst for green chemical manufacturing for industry. Because of nano size (high surface area) the contact between the reactant and catalyst increases dramatically (this phenomenon is close to the homogeneous catalysis). The insolubility of catalyst in the reaction, solvent makes catalyst heterogeneous and hence can be separated out easily from the reaction mixture (this phenomenon is close to the heterogeneous catalysis) [35]. Catalysis is one of the pioneer applications of nanoparticles. Various types of elements and materials such as aluminum, iron, titanium dioxide, clays and silica all have been used as catalyst in nanoscale for many years.

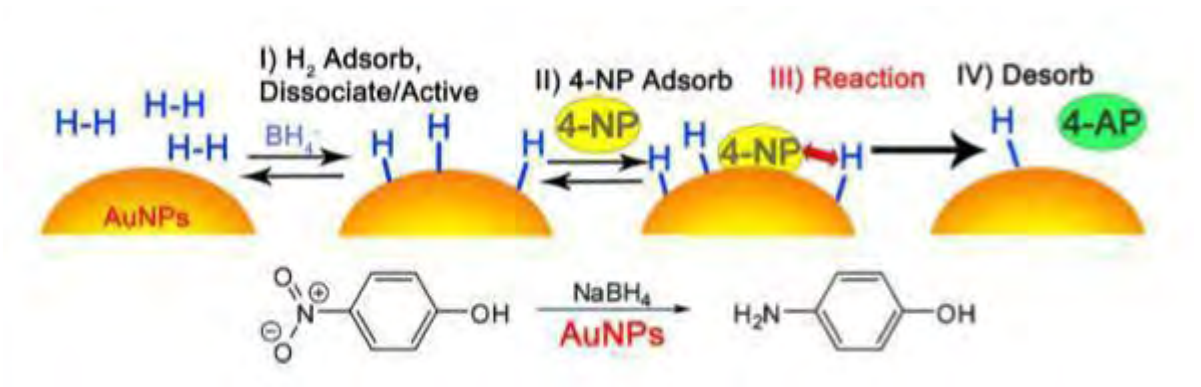

Figure 2.5 Mechanistic model of the reduction of 4-NP by borohydride in the

presence of gold nanocatalyst.

2.6.1 Activity of nanocatalysts

The appropriate reason for its tremendous catalytic behavior showing by NPs even has not been understood. The large surface area of NPs has straight forward positive effect on the rate of the reaction. Structure and shape-based properties any materials and its nanoscale can also effect on catalytic activity of a material. All of these advantages of NPs will enable industrial chemical reactions to become more resource efficient, consume less energy, and produce less waste which helps to counter the environmental impact caused by our reliance on chemical processes [36]. Figure 2.6 represents the basic difference between the bulk catalysis and catalysis shown by nanoscale materials. In recent years, noble metal nanoparticles have tensed boundless attention because of their excellent catalytic properties and potential application, such as organic synthesis, fuel cells and environmental protection [37]. NPs-based catalysts are usually heterogeneous catalyst broken up into metal nanoparticles in order to speed up the catalytic process. Metal NPs have a higher surface area so, there is increased catalytic activity because more catalytic reaction can occur at the same time. Nanoparticle catalyst can also be easily separated and recycled [38], can play two different rules in catalytic process: they can be spot and support of catalysis processes [39].

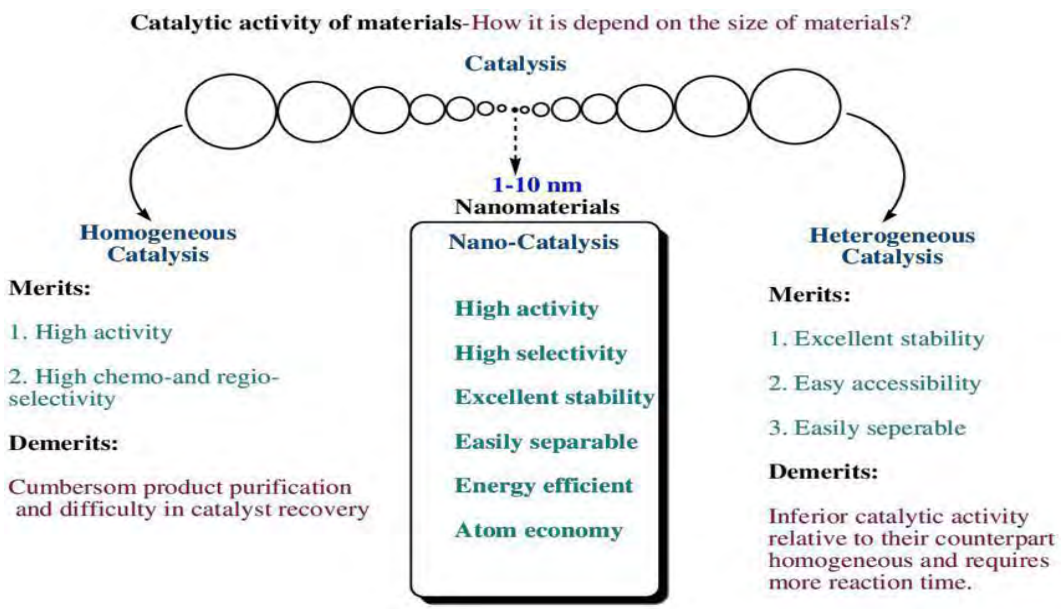

Figure 2.6 Comparative efficiency of homogeneous, heterogeneous and nanocatalysis

2.7 Nobel Metals as Nanocatalysts

Noble metal nanoparticles have attracted huge attention owing to their excellent catalytic properties and their potential applications to remove the organic dyes and hazardous chemicals. Metal nanoparticles are versatile materials that can be used in applications such as environmental remediation, energy, medical technology and water treatment [40]. Therefore, development of easy and fast method for the degradation of organic dye is a challenging job for environmental chemists. Recently, noble metal NPs such as gold, silver, palladium, platinum has been used for the degradation of various organic dyes [41].

2.7.1 AgNPs

AgNPs are very important due to their low cost, high photostability, abundance, environmentally benign nature and size and shape-dependent catalytic activities compared with the gold, palladium and all of the other metal NPs [42]. According to literature, AgNPs have various kinds of shapes. Among those shapes, preparation of quasi-spherical AgNPs has been attracted a lot of research interested due to its extravagant catalytic activity. Scientific repor ts attribute that the utilization of additives such as polymers, oligoprolines, peptides and surfactant is a good approach to fabricate quasi-spherical AgNPs in the presence of reducing agents[43].

2.7.2 Pt NPs

Due to the quite high chemical stability and catalytic activity, Pt nanomaterials have been widely used in many fields, especially in catalysis. The chemical properties of Pt are inactive and stable in air and moisture. Their existing partially-full d orbit in the outer layer of Pt results in it being easy to form complexes and some intermediates with high activity. Consequently, Pt is one of the most significant catalytic materials. Early in 1831, as catalysts, Pt had been successfully applied to the synthesis of sulfuric acid. From then on, Pt-based catalysts have attracted more and more researchers because of their excellent catalytic activity, selectivity and stability. They play an important role in a wide field of medicine, environmental protection, energy, petroche micals and fine chemicals. In 2009, Grimes and coworkers investigated nitrogen-doped titania nanotube arrays which were loaded with both Cu and Pt nanoparticles

and successfully used the catalysts for high-rate solar photo catalytic conversion of CO_2 and water vapor to hydrocarbon fuels [44]. Pt nanocatalysts for the reduction of p-nitro phenol have been also reported much more, such as the Pt nanoparticles decorated on reduced graphene oxide by the simultaneous reduction of graphene oxide and the metal ions in Mg/acid medium, dendrimer-templated and reverse micro emulsion Pt nanoparticles and reduced graphene oxide supported porous PtAu alloyed nanoflowers [45].

2.7.3 AuNPs

AuNPs based nanomaterials used as catalyst have shown highly active catalytic properties in many reactions, such as selective hydrogenation of organic molecules, carbon monoxide (CO) oxidation, and the water-gas shift reaction. The catalytic activity of AuNPs is strongly dependent on their surface chemistry. Among various nanomaterials, gold nanoparticles (AuNPs) have attracted considerable attention because of their unique physical and chemical properties and potential technological applications. Unlike bulk Au with its familiar yellow color, when the size of Au reaches nanoscale dimensions, its color changes to ruby red or purple (Figure 2.7) due to the absorption of the light at certain wavelengths, e.g., 520 nm (green light[46-48].

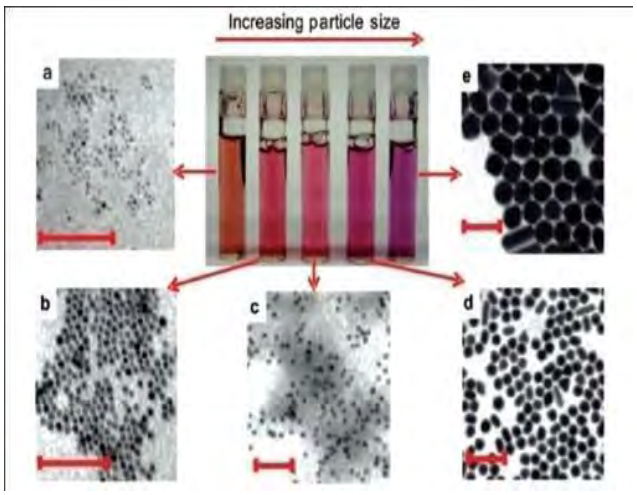

Figure 2.7 Photographs of aqueous solutions of AuNPs as a function of increasing dimensions. Corresponding transmission electron microscopy (TEM) images of the particles.

2.8Stability of Metal Nanoparticles (MNPs)

Though NPs have wide range of applications in various fields but these applications are limited due to its aggregation properties. Because of the high surface energy of NPs usually causes extensive aggregation[49, 50]. In some former method capping agents have been used to get uniform dispersed composite NPs. But capping agents require severely limit the catalytic activity of NPs. To overcome this type of problem, stabilizers and supporting materials have typically been used to obtain homogeneously distributed samples[28, 29]. Therefore, the use of high surface area materials as supports is a promising strategy for the fabrication of ultrafine and well-defined noble metal NPs that not only function as barriers to prevent encapsulated NPs from coalescing but also improve the chemical and thermal stability and enhance the electrical conductivity of functional materials. Various noble metal based catalytic systems has been developed, such as Au@ZrO2, Au@Carbon and Pt-decorated carbon composites[51]. For example, the Au@Carbon core-shell catalyst exhibits excellent catalytic properties, and it can catalyze the reduction of 4-nitrophenol (4-NP) by $NaBH_4$ to 4-aminophenol (4-AP) within 5 min at room temperature [52]. The facile and green synthesis of novel metal-NP catalysts that exhibit further improved catalytic activity remains a challenge.

2.9 Supporting Materials for Nano Particles

2.9.1 Graphene oxide (GO)

From the above- mentioned metal NPs activity, it is obvious that there is a need for a material thatcan hold metal NPs and make them more effective. There is some basic hindrance in the metal NPs activity [53]. Large scale aggregation of metal NPs is one of the main reasons for the use supporting materials. The high surface energy of metal NPs is the cause of their aggregation. To stop their aggregation and make them isolated metal NPs, high surface area supporting materials is needed [28]. Surface active materials are obvious choice for this kind of purpose. Surface active materials such as carbon-based nanomaterials, especially carbon aerogels carbon nanotubes (CNTs), graphene and their composites, represent promising type materials for this purpose. The nature of the high-surface-area materials, including their microstructure, surface chemical properties, and physical properties, is closely related to the growth of MNPs andtheir

properties [54].Moreover, by virtue of pores with well-defined size, MNPs within crystalline matrices, such as MOFs, could potentially serve as size- and/or shape-selective heterogeneous catalysts [55]. The remarkable properties of MNPs supported by high-surface-area materials have attracted a surge of interest and investment and are stimulating the emergence of innovative industrial applications in catalysis.

Graphene is one of the common materials for the purpose, consists of a o ne-atom-thick planar sheet comprising an sp^2-bonded carbon structure, is a novel material that has emerged as a rapidly rising star in the field of material science [56, 57]. Graphite oxide, formerly called graphitic oxide or graphitic acid, is a compound of carbon, oxygen, and hydrogen in variable ratios, obtained by treating graphite with strong oxidizers. The maximally oxidized bulk product is a yellow solid with C: O ratio between 2.1 and 2.9 that retains the layer structure o f graphite but with much larger and irregular spacing. The bulk material disperses in basic solutions to yield monomolecular sheets, known as graphene oxide by analogy to graphene, the single- layer form of graphite. One specific branch of graphene research deals with graphene oxide (GO). Recently, GO has attracted much research interest for its outstanding electrical, thermal, and mechanical properties [58, 59]. GO has 2-D structure with high surface area (theoretically 2630 m^2/g for single- layer graphene) and oxygen containing rich functional groups such as carboxylic, hydroxyl and epoxide groups, which confirms the availability of further modification [56, 60,61]. Graphene oxide sheets have been used to prepare strong paper-like materials, membranes, thin films, and composite materials. GO have two important properties:

i. It can be produced from cheap, easily available graphite, with high yield.

ii. It is highly hydrophilic, so it can be dispersed in an aqueous medium. This helps transport and storage in large scale applications.

For these reasons, GO is still an important topic of research despite its inferiority to pure graphene.

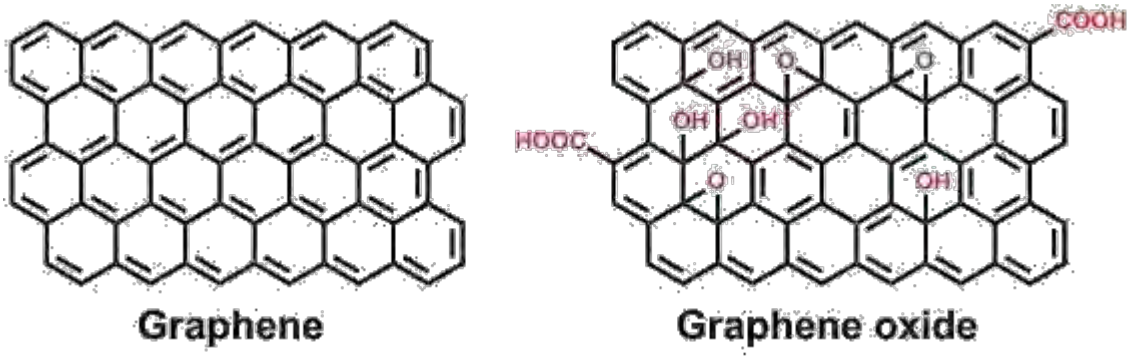

Figure 2.8 Comparison of graphene and graphene oxide structure.

2.9.2 Magnetic graphene oxide (MGO)

In nature, iron oxides exist in many forms like magnetite (Fe3O4), hematite (α-Fe2O3) and maghemite (γ-Fe2O3). Among these oxides Fe3O4 particles are more demandable due to surface efficiency. It is reported that the surface area of iron-oxide-based magnetic materials decreased their response to external magnetic field making it difficult to recover the adsorbents after treatment has been completed. On the other hand, it has also been reported that the adsorption capacities of adsorbents rely largely on the available surface areas, and the increase of the surface area is normally obtained by the decrease of the particle size of adsorbents. As a result, there is a need to synthesize such absorbents with proper particle size for the removal of dye or heavy metals from industrial wastewater. Up to date, there are many methods to synthesize iron-oxide nanoparticle. The most common methods include co-precipitation, hydrothermal synthesis, thermal decomposition, sol- gel method, and colloidal chemistry method. Among these methods, co-precipitation has proven to be the most promising method for the production of iron oxide nanoparticles as the procedure is relatively simple and the particles can be obtained with controlled particle size.

Recently, more attention has been paid to the functionalization of carbon nanotubes (CNTs) with various inorganic nanoparticles such as metals, metal oxides for further improving their properties and extending their applications in various fields of technology [62]. Among these multifunctional composites, magnetic CNTs composites have been emerging to be an interesting area of advanced research owing to their potential applications in microwave absorption, electrochemical biosensor [63].

2.9.3 Polydopamine

To apply magnetic GO in some applications, much work has been done to functionalize the magnetic GO surface with another phase to enhance compatibility and improve stability. Among all materials, silica as a protecting shell was utilized to coat the magnetic carbon nanotube [64]. Although there have been lots of reports about successful synthesis of silica-coated magnetic GO, little work has been done to functionalize with organic coating. In the case of polymer shell layers, DA has received significant attention as a candidate material because of its unique coating quality and functionality [65]. It has been reported that the self-polymerization of dopamine could form stable coating on the surface of inorganic and organic materials in comparison to the other coating techniques [66]. Besides its biocompatibility and adhesiveness, the DA coatings have the other attractive features: DA coatings can serve as a versatile platform for secondary surface- mediated reactions, leading to tailoring of coatings for diverse uses. More importantly, DA has been shown to be an effective carbon source for the formation of carbon-coated materials [67].

References

[1] G. D. Yadav, and J. J. Nair, "Sulfated zirconia and its modified versions as promising catalysts for industrial processes," *Microporous and Mesoporous Materials,* vol. 33, pp. 1-48, (1999).

[2] W. Vermeiren, and J. P. Gilson, "Impact of Zeolites on the Petrole um and Petrochemical Industry," *Topics in Catalysis,* vol. 52, pp. 1131-1161, (2009).

[3] Y. Chaohe, C. Xiaobo, Z. Jinhong *et al.*, "Advances of two-stage riser catalytic cracking of heavy oil for maximizing propylene yield (TMP) process," *Applied Petrochemical Research,*
vol. 4, pp. 435-439, (2014).

[4] M. Sharifzadeh, L. Wang, and N. Shah, "Decarbonisation of olefin processes using biomass pyrolysis oil," *Applied Energy,* vol. 149, pp. 404-414, (2015).

[5] P. T. Wolczanski, and P. J. Chirik, "A Career in Catalysis: Jo hn E. Bercaw," *ACSCatalysis,* vol. 5, pp. 1747-1757, (2015).

[6] K.-i. Tanaka, "Unsolved problems in catalysis," *Catalysis Today,* vol. 154, no. 1, pp. 105-112, 2010/09/01/, 2010.

[7] D. Kumar Dutta, B. Jyoti Borah, and P. Pollov Sarmah, "Recent Advances in Metal Nanoparticles Stabilization into Nanopores of Montmorillonite and Their Catalytic Applications for Fine Chemicals Synthesis," *Catalysis Reviews,* vol. 57, pp. 257-305, (2015).

[8] T. Yasukawa, A. Suzuki, H. Miyamura *et al.*, "Chiral Metal Nanoparticle Systems as Heterogeneous Catalysts beyond Homogeneous Metal Complex Catalysts for Asymmetric Addition of Arylboronic Acids to α,β-Unsaturated Carbonyl Compounds," *Journal of theAmerican Chemical Society,* vol. 137, pp. 6616-6623, (2015).

[9] S. Zhang, J. Li, W. Gao *et al.*, "Insights into the effects of surface properties of oxides on the catalytic activity of Pd for C–C coupling reactions," *Nanoscale,* vol. 7, pp. 3016-3021, (2015).

[10] S. Zhang, X. Shen, Z. Zheng *et al.*, "3D graphene/nylon rope as a skeleton for noble metal nanocatalysts for highly efficient heterogeneous continuous-flow reactions," *Journal ofMaterials Chemistry A,* vol. 3, pp. 10504-10511, (2015).

[11] M. Xiao, L. Feng, J. Zhu *et al.*, "Rapid synthesis of a PtRu nano-sponge with different surface compositions and performance evaluation for methanol electrooxidation," *Nanoscale,* vol. 7, pp. 9467-9471, (2015).

[12] L. Ai, and J. Jiang, "Catalytic reduction of 4- nitrophenol by silver nanoparticles stabilized on environmentally benign macroscopic biopolymer hydrogel," *Bioresource Technology,* vol. 132, pp. 374-377, (2013).

[13] B. Subash, B. Krishnakumar, M. Swaminathan *et al.*, "Highly Efficient, Solar Active, and Reusable Photocatalyst: Zr-Loaded Ag–ZnO for Reactive Red 120 Dye Degradation with Synergistic Effect and Dye-Sensitized Mechanism," *Langmuir,* vol. 29, pp. 939-949, (2013).

[14] E. Karaoğlu, U. Özel, C. Caner *et al.*, "Synthesis and characterization of NiFe2O4–Pd magnetically recyclable catalyst for hydrogenation reaction," *Materials Research Bulletin,* vol. 47, no. 12, pp. 4316-4321, (2012).

[15] E. Karaoğlu, U. Özel, C. Caner *et al.*, "Synthesis and characterization of NiFe2O4–Pd magnetically recyclable catalyst for hydrogenation reaction," *Materials Research Bulletin,* vol.47, pp. 4316-4321, (2012).

[16] Y. Junejo, Sirajuddin, A. Baykal *et al.*, "A novel green synthesis and characterization of Ag NPs with its ultra-rapid catalytic reduction of methyl green dye," *Applied Surface Science,* vol. 290, pp. 499-503, (2014).

[17] J. Cai, Y. Huang, B. Huang *et al.*, "Enhanced activity of Pt nanoparticle catalysts supported on manganese oxide-carbon nanotubes for ethanol oxidation," *International Journalof Hydrogen Energy,* vol. 39, pp. 798-807, (2014).

[18] G. C. Bond, "Gold: a relatively new catalyst," *Catalysis Today,* vol. 72, pp. 5-9, (2002).

[19] R. Dai, J. Chen, J. Lin *et al.*, "Reduction of nitro phenols using nitroreductase from E. coli in the presence of NADH," *Journal of Hazardous Materials,* vol. 170, pp. 141-143, (2009).

[20] T. Sugimura, and M. Nagao, "Carcinogenic, Mutagenic, and Comutagenic Aromatic Amines in Human Foods," *Natl Cancer Inst Monogr,* vol. 58, pp. 27-33, (1981).

[21] Y. Shiraishi, T. Hirai, and I. Komasawa, "Photochemical Denitrogenation Processes for Light Oils Effected by a Combination of UV Irradiation and Liquid−Liquid Extraction," *Industrial & Engineering Chemistry Research,* vol. 39, pp. 2826-2836, (2000).

[22] M. Nasrollahzadeh, M. Atarod, and S. M. Sajadi, “Green synt hesis of the Cu/Fe3O4 nanoparticles using Morinda morindoides leaf aqueous extract: A highly efficient magnetically
separable catalyst for the reduction of organic dyes in aqueous medium at room temperature,” *Applied Surface Science,* vol. 364, pp. 636-644, (2016).

[23] P. Kovacic, and R. Somanathan, “Nitroaromatic compounds: Environmental toxicity, carcinogenicity, mutagenicity, therapy and mechanism,” *Journal of Applied Toxicology,* vol. 34, no. 8, pp. 810-824, (2014).

[24] M. Mali, M. Michela Dell'Anna, P. Mastrorilli *et al.*, *Identification of hot spots withinharbour sediments through a new cumulative hazard index. Case study: Port of Bad, Italy*,(2016).

[25] A. Nezamzadeh- Ejhieh, and S. Khorsandi, “Photocatalytic degradation of 4-nitrophenol with ZnO supported nano-clinoptilolite zeolite,” *Journal of Industrial and EngineeringChemistry,* vol. 20, pp. 937-946, (2014).

[26] P. Jiang, J. Zhou, A. Zhang *et al.*, “Electrochemical degradation of p- nitrophenol with different processes,” *Journal of Environmental Sciences,* vol. 22, pp. 500-506, (2010).

[27] R. Begum, R. Rehan, Z. H. Farooqi *et al.*, “Physical chemistry of catalytic reduction of nitroarenes using various nanocatalytic systems: past, present, and future,” *Journal ofNanoparticle Research,* vol. 18, pp. 231, (2016).

[28] M.-P. Pileni, “The role of soft colloidal templates in controlling the size and shape of inorganic nanocrystals,” *Nature Materials,* vol. 2, pp. 145-150, (2003).

[29] O. M. Wilson, R. W. J. Scott, J. C. Garcia-Martinez *et al.*, “Synthesis, Characterization, and Structure-Selective Extraction of 1−3-nm Diameter AuAg Dendrimer-Encapsulated Bimetallic Nanoparticles,” *Journal of the American Chemical Society,* vol. 127, pp. 1015-1024, (2005).

[30] A. Casitas, and X. Ribas, “The role of organometallic copper(iii) complexes in homogeneous catalysis,” *Chemical Science,* vol. 4, pp. 2301-2318, (2013).

[31] Y. Zhang, S. Pang, Z. Wei *et al.*, “Synthesis of a molecularly defined single-active site heterogeneous catalyst for selective oxidation of N-heterocycles,” vol. 9, pp. 1465, (2018).

[32] E. Marlina, S. Nee Goh, T. Yeong Wu *et al.*, *Evaluation on the Photocatalytic Degradation Activity of Reactive Blue 4 using Pure Anatase Nano-TiO2*, (2015).

[33] A. Mills, “Heterogeneous redox catalysts for oxygen and chlorine evolution,” *Chemical Society Reviews,* vol. 18, pp. 285-316, (1989).

[34] S. J. Benkovic, and S. Hammes-Schiffer, “A Perspective on Enzyme Catalysis,” *Science,*vol. 301, pp. 1196, (2003).

[35] K. Yan, G. Wu, C. Jarvis *et al.*, “Facile synthesis of porous microspheres composed of TiO2 nanorods with high photocatalytic activity for hydrogen production,” *Applied CatalysisB: Environmental,* vol. 148-149, pp. 281-287, (2014).

[36] K. Yan, C.Jarvis, T.Lafleur et *al.*, “Novel synthesis of Pd nanoparticles for hydrogenation of biomass-derived platform chemicals showing enhanced catalytic performance,” *RSC Advances,* vol. 3, pp. 25865-25871, (2013).

[37] Y. Nishihata, J. Mizuki, T. Akao *et al.*, “Self-regeneration of a Pd-perovskite catalyst for automotive emissions control,” *Nature,* vol. 418, pp. 164-167, (2002).

[38] T. Fukui, K. Murata, S. Ohara *et al.*, “Morphology control of Ni–YSZ cermet anode for lower temperature operation of SOFCs,” *Journal of Power Sources,* vol. 125, pp. 17-21, (2004).

[39] N. End, and K.-U. Schöning, "Immobilized Catalysts in Industrial Research and Application," *Immobilized Catalysts: Solid Phases, Immobilization and Applications*, A. Kirschning, ed., pp. 241-271, Berlin, Heidelberg: Springer Berlin Heidelberg, (2004).

[40] M. Amini, H. Naslhajian, and S. M. F. Farnia, “V-doped titanium mixed oxides as efficient catalysts for oxidation of alcohols and olefins,” *New Journal of Chemistry,* vol. 38, pp.1581-1586, (2014).

[41] Z. Xiong, L. L. Zhang, J. Ma *et al.*, “Photocatalytic degradation of dyes over graphene–gold nanocomposites under visible light irradiation,” *Chemical Communications,* vol. 46, pp. 6099-6101, (2010).

[42] C. Milone, R. Ingoglia, M. L. Tropeano *et al.*, “First example of selectivehydrogenationof unconstrained α,β-unsaturated ketone to α,β-unsaturated alcohol by molecular hydrogen,” *Chemical Communications,* vol. 45, pp. 868-869, (2003).

[43] M. Rycenga, C. M. Cobley, J. Zeng *et al.*, “Controlling the Synthesis and Assembly of Silver Nanostructures for Plasmonic Applications,” *Chemical Reviews,* vol. 111, pp. 3669-3712, (2011).

[44] R. Zong, X. Wang, S. Shi *et al.*, “Kinetically controlled seed- mediated growth of narrow dispersed silver nanoparticles up to 120 nm: secondary nucleation, size focusing, and Ostwaldripening,” *Physical Chemistry Chemical Physics,* vol. 16, pp. 4236-4241, (2014).

[45] O. K. Varghese, M. Paulose, T. J. LaTempa *et al.*, "High-Rate Solar Photocatalytic Conversion of CO2 and Water Vapor to Hydrocarbon Fuels," *Nano Letters,* vol. 9, pp. 731-737, (2009).

[46] P. Song, L.-L. He, A.-J. Wang *et al.*, "Surfactant-free synthesis of reduced graphene oxide supported porous PtAu alloyed nanoflowers with improved catalytic activity," *Journal ofMaterials Chemistry A,* vol. 3, pp. 5321-5327, (2015).

[47] S. K. Ghosh, and T. Pal, "Interparticle Coupling Effect on the Surface Plasmon Resonance of Gold Nanoparticles: From Theory to Applications," *Chemical Reviews,* vol. 107, pp. 4797-4862, (2007).

[48] A. Corma, and H. Garcia, "Supported gold nanoparticles as catalysts for organic reactions," *Chemical Society Reviews,* vol. 37, pp. 2096-2126, (2008).

[49] P. Li, Z. Wei, T. Wu *et al.*, "Au−ZnO Hybrid Nanopyramids and Their Photocatalytic Properties," *Journal of the American Chemical Society,* vol. 133, pp. 5660-5663, (2011).

[50] S. Chen, Z. Wei, X. Qi *et al.*, "Nanostructured Polyaniline-Decorated Pt/C@PANI Core–Shell Catalyst with Enhanced Durability and Activity," *Journal of the American ChemicalSociety,* vol. 134, pp. 13252-13255, (2012).

[51] P. M. Arnal, M. Comotti, and F. Schüth, "High- Temperature-Stable Catalysts by HollowSphere Encapsulation," *Angewandte Chemie International Edition,* vol. 45, pp. 8224-8227, (2006).

[52] R. Liu, S. M. Mahurin, C. Li *et al.*, "Dopamine as a Carbon Source: The Controlled Synthesis of Hollow Carbon Spheres and Yolk-Structured Carbon Nanocomposites," *Angewandte Chemie International Edition,* vol. 50, no. 30, pp. 6799-6802, (2011).

[53] Y. Li, Y. Li, E. Zhu *et al.*, "Stabilization of High-Performance Oxygen Reduction Reaction Pt Electrocatalyst Supported on Reduced Graphene Oxide/Carbon Black Composite," *Journal of the American Chemical Society,* vol. 134, pp. 12326-12329, (2012).

[54] Z. Li, J. Liu, C. Xia *et al.*, "Nitrogen-Functionalized Ordered Mesoporous Carbons as Multifunctional Supports of Ultrasmall Pd Nanoparticles for Hydrogenation of Phenol," *ACSCatalysis,* vol. 3, pp. 2440-2448, (2013).

[55] W. Zhang, G. Lu, C. Cui *et al.*, "A Family of Metal-Organic Frameworks Exhibiting Size-Selective Catalysis with Encapsulated Noble-Metal Nanoparticles," *Advanced Materials,* vol. 26, pp. 4056-4060, (2014).

[56] A. K. Geim, and K. S. Novoselov, "The rise of graphene," *Nat Mater,* vol. 6, no. 3, pp. 183-91, Mar, (2007).

[57] E. C. H. Sykes, "Graphene goes undercover," *Nature Chemistry,* vol. 1, pp. 175, (2009).

[58] A. A. Balandin, S. Ghosh, W. Bao *et al.*, "Superior Thermal Conductivity of Singlelayer Graphene,'' Nano Letters, vol. 8, pp. 902-907, (2008).

[59] K. I. Bolotin, K. J. Sikes, Z. Jiang *et al.*, "Ultrahigh electron mobility in suspended graphene," *Solid State Communications,* vol. 146, pp. 351-355, (2008).

[60] M. D. Stoller, S. Park, Y. Zhu *et al.*, "Graphene-Based Ultracapacitors," *Nano Letters,* vol. 8, pp. 3498-3502, (2008).

[61] S. Park, and R. S. Ruoff, "Chemical methods for the production of graphenes," *NatureNanotechnology,* vol. 4, pp. 217, (2009).

[62] M. Mazloumi, S. Shadmehr, Y. Rangom *et al.*, "Fabrication of Three-Dimensional Carbon Nanotube and Metal Oxide Hybrid Mesoporous Architectures," *ACS Nano,* vol. 7, pp. 4281-4288, (2013).

[63] Z. Wang, L.Wu, J. Zhou *et al.*, "Magnetite Nanocrystals on Multiwalled Carbon Nanotubes as a Synergistic Microwave Absorber," *The Journal of Physical Chemistry C,* vol. 117, pp. 5446-5452, (2013).

[64] J. Sui, J. Li, S. Yang *et al.*, "A facile method to fabricate superparamagnetic γ-Fe2O3/silica nanotubes using multi-walled carbon nanotubes as template," *Materials Letters,* vol. 100, pp. 32-35, (2013).

[65] Y. Liu, K. Ai, and L. Lu, "Polydopamine and Its Derivative Materials: Synthesis a nd Promising Applications in Energy, Environmental, and Biomedical Fields," *Chemical Reviews,* vol. 114, pp. 5057-5115, (2014).

[66] H. Lee, S. M. Dellatore, W. M. Miller *et al.*, "Mussel-Inspired Surface Chemistry for Multifunctional Coatings," *Science,* vol. 318, pp. 426, (2007).

[67] R. Liu, S. M. Mahurin, C. Li *et al.*, "Dopamine as a Carbon Source: The Controlled Synthesis of Hollow Carbon Spheres and Yolk-Structured Carbon Nanocomposites," *Angewandte Chemie International Edition,* vol. 50, pp. 6799-6802, (2011).

CHAPTER 3

Experimental

3.1 Materials and Instruments

3.1.1 Chemical and reagents

The chemicals and reagents used in this research were analytical grade and used without further purification. De- ionized (DI) water was used as a solvent to prepare most of the solutions of this work. Purity and CAS Registry number of all studied materials as tabular form. The chemicals and reagents which were used in this research are given below:

i. Graphite flake (325 mesh), (Merck, Germany)
ii. Potassium permanganate (Merck, Germany)
iii. Sulfuric acid (Merck, Germany)
iv. Hydrogen peroxide (Sigma-Aldrich)
v. Ferrous chloride 4H2O (Sigma Aldrich)
vi. Ferric chloride 6H2O (Sigma Aldrich)
vii. 2-amino-2-hydroxymethylpropane-1, 3-diol (Tris) (Sigma-Aldrich)
viii. Dopamine hydrochloride (Sigma-Aldrich)
ix. Hydrogen tetrachloroaurate hydrate (HAuCl4·4H2O)
x. Silver nitrate (analytical grade)
xi. Ammonia solution (25%) (Merck, Germany)
xii. p-nitrophenol
xiii. NaBH4

3.1.2 Instruments

Synthesis, characterization and data analysis were performed by using the following instruments

i. Fourier Transform Infrared Spectrophotometer (SHIMADZU FTIR-8400)
ii. Field Emission Scanning Electron Microscopy (JSM-7600F, Tokyo, Japan)
iii. UV-visible Spectrophotometer (Shimadzu-1800)
iv. X-ray Diffractometer (Philips, Expert Pro, Holland)
v. Thermo gravimetric analyser (TGA 50-H)
vi. Centrifuge machine (Hettich, Universal 16A)
vii. pH meter (Hanna, HI 8424, Romania)
viii. Digital Balance (AB 265/S/SACT METTLER, Toleto, Switzerland)
ix. Freeze dryer (Heto FD3)
x. Oven (Lab Tech, LDO-030E)
xi. Vacuum oven
xii. Hot plate

3.2 Method of Preparation

3.2.1 Preparation of Graphene Oxide (GO)

Graphene oxide was synthesized from synthetic graphite powder according to the modified Hummers method [1]. 2g of graphite powder (Alfar Aesar, 99. 999% purity, 200 mesh) was put into concentrated H_2SO_4 (12mL) and HNO_3 (8mL) at 80°C. The mixture was kept at that temperature for 8h using a water-bath. After cooling to room temperature, the mixture was diluted with 0.5L of de-ionized (DI) water and left overnight. Then, the mixture was filtered and washed with DI water. The product was dried under ambient conditions overnight. After that the treated graphite powder (1g), $NaNO_3$ (1. 03g), and concentrated H_2SO_4 (62g) were placed in a flask. Then, 4.5g of $KMnO_4$ was slowly added under stirring and the temperature of the mixture was kept to below 20°C for 2h. After further vigorous stirring for 2 days at room temperature, the reaction was terminated by the addition of DI water (140mL) and 30% H_2O_2

solution (2.5mL). The mixture was filtered and washed by repeated centrifugation and filtration, first with 1M HCl aqueous solution and then with DI water. DI water (50mL) was added to the final product, which was subjected to ultrasonication. The obtained mixture was dialyzed through semi-permeable membranes for one week to remove the remaining metal species. Finally, the resulting solid was dried in air and can use for further modification.

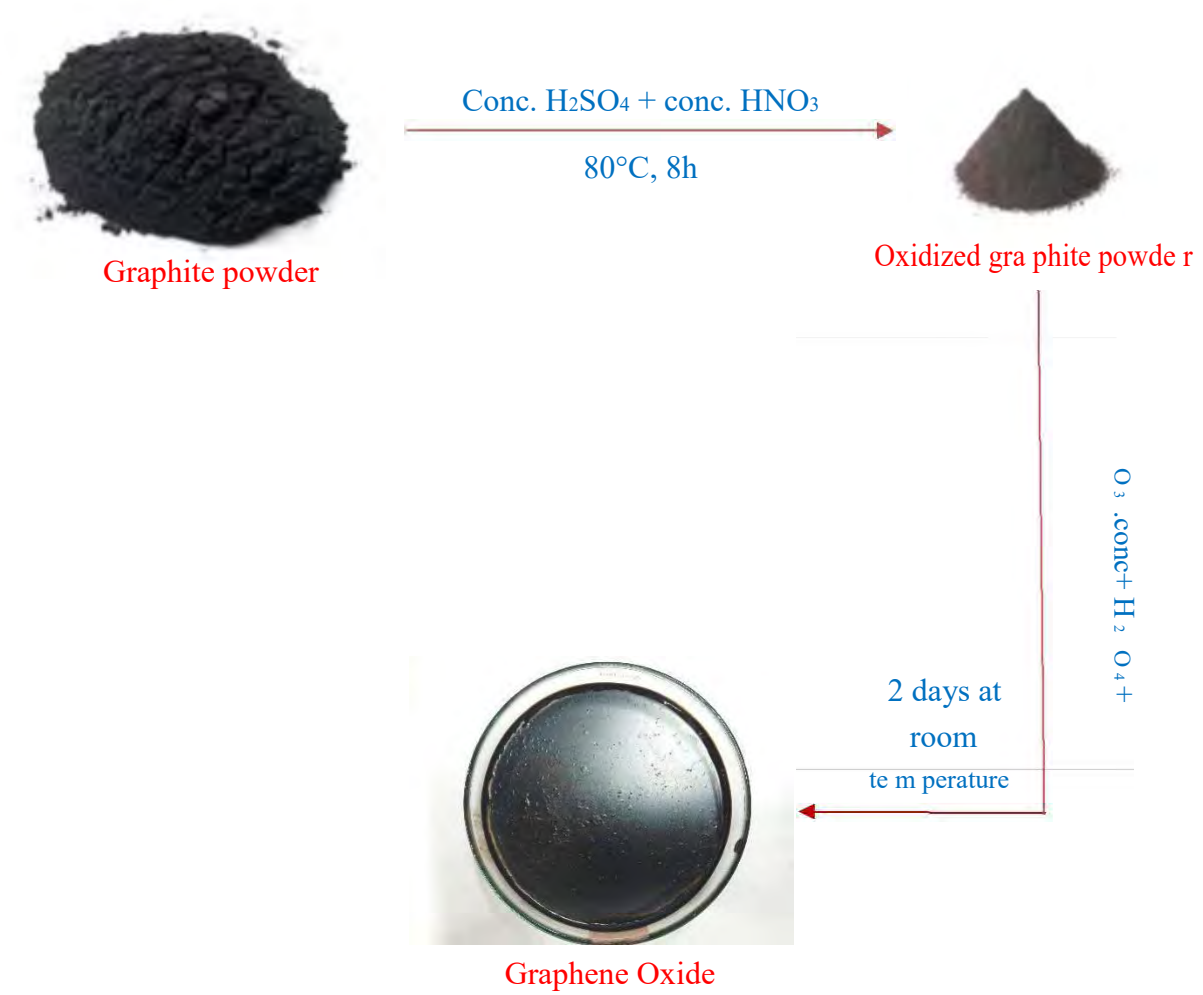

Figure 3.1 Schematic illustration of graphene oxide (GO) preparation.

3.2.2 Preparation of Magnetic Graphene Oxide (MGO)

MGO was synthesized following a modified co-precipitation method [2]. The procedure of a typical synthesis experiment is as follows. Firstly, 100mg GO was dispersed into 100mL of DI water by ultrasonication. Then the GO dispersion was added into a 250mL three- necked flask

and stirred vigorously. Secondly, $FeCl_3.6H_2O$ (0.4095g) and $FeCl_2.4H_2O$ (0.147g) were dissolved in DI water (12mL) and the solution was dropped into the flask containing GO dispersion under severe agitation for 20min. Afterward, the mixture was heated to 50°C and the pH was adjusted to 10 with the observation of black precipitation. The solution was further heated to 85°C and the heat was maintained for an hour. The as-prepared MGO was magnetically separated and washed for more than 3 times. Finally, black MGO powder was obtained by drying.

3.2.3 Fabrication of Polydopamine on MGO (MGO-PDA)

A thin layer of polydopamine (PDA) was coated onto MGO [3]. 60mg of GO and 15mg of dopamine hydrochloride were dispersed in 100mL of 10mM Tris-HCl (pH 8.5) buffer and then sonicated for 30min. Afterward, the mixture was stirred at 60°C for 24h. The resultant product was separated and collected with a magnet, followed by washing with deionized water 3 times.

3.2.4 Preparation of MGO-PDA@Au nanocatalyst

In a typical preparation of MGO-PDA@Au, 100mg of MGO-PDA NPs were suspended in $HAuCl_4$ aqueous solution (80mL) and the mixture was stirred for 24h at room temperature. The resultant nanocomposite was separated and rinsed with deionized water for at least three times, and then dried under vacuum oven at 50°C for further use [4].

3.2.5 Preparation of MGO-PDA@Ag nanocatalyst

Preparation of MGO-PDA@Ag, 80mg of MGO-PDA NPs was added with 2% ammonium $AgNO_3$ aqueous solution (10mg/mL) and the mixture was stirred for 12h at room temperature in rotator shaker. The resultant nanocomposite was separated and rinsed with deionized water and ethanol for at least three times, and then dried under vacuum oven at 50°C for further use [5].

3.3 Sample Characterization

3.3.1 Fourier Transform Infrared (FTIR) analysis

The infrared spectra of the graphene oxide (GO), magnetic graphene oxide (MGO), poly dopamine coated MGO (MGO-PDA), gold-coated catalyst (MGO-PDA@Au) and silver-coated catalyst (MGO-PDA@Ag) were recorded on an FTIR spectrometer in the region of 4000 – 500 cm^{-1}. All the 4 samples had dried. A small portion of samples were taken into vial and oven-dried at 60 °C to confirm their dryness. GO flake is very strong so it was ground into a mortar with a pestle to get GO powder. The other four samples were not ground because they were physically granule/powder in shape after completely drying. The powder mixture was then compressed in a metal holder under a pressure of 8–10 tons to make a pellet. The pellet was then placed in the path of IR beam for measurements.

3.3.2 Scanning Electron Microscopy (SEM)

The surface morphology of the synthesized magnetic graphene oxide (MGO), poly dopamine coated magnetic graphene oxide (MGO-PDA), gold-coated catalyst (MGO-PDA@Au) and silver-coated catalyst (MGO-PDA@Ag) was adopted using Scanning Electron Microscopy (SEM). The completely air-dried samples were put on a conducting carbon strip. The sample loaded strip was then mounted to a chamber that evacuated to ~ 10^{-3} to 10^{-4} torr and then a very thin platinum layer (~few nanometers thick) were sputtered on the sample to ensure the conductivity of the sample surface. The sample was then placed in the main SEM chamber to view its surface. The microscope was operated at an accelerating voltage of 5.0 kV. The system was computer interfaced and thus provides recording of the surface images in the computer file for its use as hard copy.

3.3.3 X-ray diffraction (XRD)

The crystallinity of magnetic graphene oxide (MGO), gold-coated catalyst (MGO-PDA@Au) and silver-coated catalyst (MGO-PDA@Ag) composite were analyzed by X-ray diffraction pattern in the powder state. The powder samples were pressed in a square aluminum sample holder (40 mm × 40 mm) with a 1 mm deep rectangular hole (20 mm × 15 mm) and pressed

against an optical smooth glass plate. The upper surface of the sample was labeled in the plane with its sample holder. The sample holder was then placed in the diffractometer.

3.3.4 Thermo Gravimetrical Analysis (TGA)

TGA is the study of weight loss of a specimen with respect to the temperature increasing. The quantities are recorded for a TGA; they are the weight, the temperature, and temperature change rate. Weight loss and weight loss rates are usually plotted for further analysis. TGA system usually consists of high precision with pans, an oven and a closed chamber. The balance must able to sustain high temperatures up to 100°C.The thermal stability of MGO - PDA, MGO-PDA@Au and MGO-PDA@Ag were studied by a thermo-gravimetric analyzer (TGA) in a nitrogen atmosphere. Approximately 3-10mg freeze-dried samples taken into an aluminum cell and heated from 27°C to 800°C at a heating rate of 10 °C/min under a nitrogen flow of 10 mL/ min. Before the data acquisition segment, the sample was equilibrated at 25°C for 5 min to obtain an isothermal condition.

3.3.5 Magnetic Property Analysis

The magnetic properties of MGO, MGO-PDA@Au and MGO-PDA@Ag were measured EV-9 Microsensor (Germany) with an applied field between -10000 and 10000 Oe at room temperature. The samples were dried in an oven overnight and then taken for analysis.

3.3.6 Reduction Experiments (MB) by $NaBH_4$

0.5 mL of fresh $NaBH_4$ aqueous solution (0. 1mol L^{-1}) was injected into 4. 5 mL of methylene blue (MB) aqueous solution (20 mgL^{-1}) under stirring. The blue color of MB gradually vanished by catalytic reduction. The reduction process was monitored by measuring the changes in the absorbance at 665nm at different times (i.e. 0 min, 1 min, 2 min, 3 min, 4 min, 5 min,6 min) with a UV−Vis spectrophotometer. Again 3 mL 4-Nitrophenol (4-NP) solution (0. 1 mM) was stirred with $NaBH_4$ solution with time interval (i.e. 0 min, 1 min, 2 min, 3 min, 4 min, 5 min,6 min etc.). The reduction process was monitored by measuring the changes in the absorbance.

3.3.7 Reduction Experiments (4-NP) by $NaBH_4$

At first 3mL of 4-nitrophenol (4-NP) (0.1mmolL^{-1}) was taken and 2mL freshly prepared $NaBH_4$ (0.1molL^{-1}) was added to it with stirring then the reduction process was monitored by measuring the changes in the absorbance at 400nm at different time interval (i.e. 0 min, 1 min, 2 min, 3 min, 4 min, 5 min, 6 min, 7 min, 8 min, 9 min, 10min……) with a UV −Vis spectrophotometer.

Again 0.5 mL of freshly prepared $NaBH_4$ aqueous solution (0.1mol L^{-1}) was injected into 4.5mL of methylene blue (MB) aqueous solution (20mgL^{-1}) under stirring. The blue color of MB gradually vanished. The reduction process was monitored by measuring the changes in the absorbance at 665nm at different times (i.e. 0 min, 1 min, 2 min, 4 min, 7 min, 10 min+) with a UV−Vis spectrophotometer.

3.3.8 Catalytic Experiments

3.3.8.1 Reduction of 4-nitrophenol (4-NP)

3 mg portion of catalyst (MGO-PDA@Au) was dispersed in 5mL of DI water. Then 3mL of 4-nitrophenol (4-NP) aqueous solution (0.1mmolL^{-1}) added to it. Subsequently, 2mL of freshly prepared $NaBH_4$ aqueous solution (0.1molL^{-1}) was injected into the solution under stirring. The yellow color of 4-NP gradually vanished by catalytic reduction in the presence of reducing agents. The catalytic process was monitored by measuring the changes in the absorbance at 400 nm at different time (i.e. 0 min, 1 min, 2 min, 3 min, 4 min, 5 min, 6 min, 7 min, 8 min, 9 min) with a UV −Vis spectrophotometer. Mainly the observation was monitored with catalyst and without catalyst. Then the same experiment was repeated with silver catalyst with the same time interval [6].

3.3.8.2 Reduction of methylene blue (MB)

At first 4.5mL of methylene blue (MB) was taken and 0.5ml freshly prepared $NaBH_4$ was added to it to monitor their catalytic process by UV spectrum. After that 3 mg portion of catalyst (MGO-PDA@Au) was dispersed in 5 mL of DI water. Then again 4.5mL of methylene blue (MB) aqueous solution ($20 mgL^{-1}$) added to it. Subsequently, 0.5mL freshly prepared $NaBH_4$ aqueous solution ($0.1 molL^{-1}$) was injected into the solution under stirring. The blue color of MB gradually faded by the catalytic reduction. The catalytic process was monitored by measuring the changes in the absorbance at 665nm at different times (i.e. 0 min, 1 min, 2 min, 3 min, 4 min, 5 min, 6 min, 7 min, 8 min, 9 min) with a UV −Vis spectrophotometer. Mainly the observation was monitored with catalyst and without catalyst. Then the same experiment was repeated with silver catalyst with same time interval [6].

References

[1] H. Tetsuka, R. Asahi, A. Nagoya *et al.*, "Optically Tunable Amino-Functionalized Graphene Quantum Dots," *Advanced Materials,* vol. 24, pp. 5333-5338, (2012).

[2] J. Zhang, M. S. Azam, C. Shi *et al.*, "Poly(acrylic acid) functionalized magnetic graphene oxide nanocomposite for removal of methylene blue," *RSC Advances,* vol. 5, pp. 32272-32282, (2015).

[3] J. Miao, H. Liu, W. Li *et al.*, "Mussel-Inspired Polydopamine-Functionalized Graphene as a Conductive Adhesion Promoter and Protective Layer for Silver Nanowire Transparent Electrodes," *Langmuir,* vol. 32, pp. 5365-5372, (2016).

[4] T. Zeng, X.- l. Zhang, H.-y. Niu *et al.*, "In situ growth of gold nanoparticles onto polydopamine-encapsulated magnetic microsphere s for catalytic reduction of nitrobenzene," *Applied Catalysis B: Environmental,* vol. 134-135, pp. 26-33, (2013).

[5] Y. Xie, B. Yan, H. Xu *et al.*, "Highly Regenerable Mussel- Inspired Fe3O4@Polydopamine-Ag Core–Shell Microspheres as Catalyst and Adsorbent for Methylene
Blue Removal," *ACS Applied Materials & Interfaces,* vol. 6, pp. 8845-8852, (2014).

[6] A. Ma, Y. Xie, J. Xu *et al.*, "The significant impact of polydopamine on the catalytic performance of the carried Au nanoparticles," *Chemical Communications,* vol. 51, pp. 1469-1471, (2015).

CHAPTER 4

RESULTS AND DISCUSSION

4.1 **Synthesis of Nanocatalyst**

In order to incorporate the magnetic properties in graphene oxide (GO), Fe_3O_4 nanoparticles were loaded on the surface of GO. $FeCl_2$ and $FeCl_3$ solution (Fe^{2+} : Fe^{3+} = 2:1) were dropped to GO suspensions as an iron source, with Fe^{2+} and Fe^{3+} ions attracted to the negatively charged oxygen atoms of GO. The solution was adjusted to alkaline condition (pH 10) and Fe_3O_4 particles were formed in situ by co-precipitation [7]. MGO-PDA was fabricated by mixing the MGO aqueous suspension with dopamine hydrochloride at pH 8. 5. However, no obvious aggregate formation was observed when MGO-PDA was dispersed in water, which is attributed to the stabilization by PDA [8]. The prevalent view is that in alkaline conditions dopamine is oxidized to dopamine quinone. The adhesion of PDA onto Fe_3O_4 surface may attribute to the formation of $COO^{-}H_3N^{+}$ ion pairs between the abundant carboxyl groups on the particle surface and the amine groups of dopamine [9]. The structure of MGO-PDA@Au nanocomposites was obtained by adding the as-prepared MGO -PDA to a $HAuCl_4$ solution and did not require extra reagents or thermal treatment
[10]. The possible mechanism of the generation and stabilization of Au NPs on PDA coating is speculated in Fig.4. 1. When MGO -PDA NPs are mixed with $HAuCl_4$ solution, Au^{3+} ions diffuse into the PDA layer and then are reduced to Au^{0} atoms in situ by the catechol groups of PDA and the catechol groups are oxidized to corresponding quinones. On the other hand the core-shell structured MGO-PDA@Ag nanocomposites were obtained by adding the as-prepared MGO-PDA with Tollen's reagent and shake for 12h [11]. Ag nanocatalyst was synthesized in same steps for the comparison with Au catalyst.

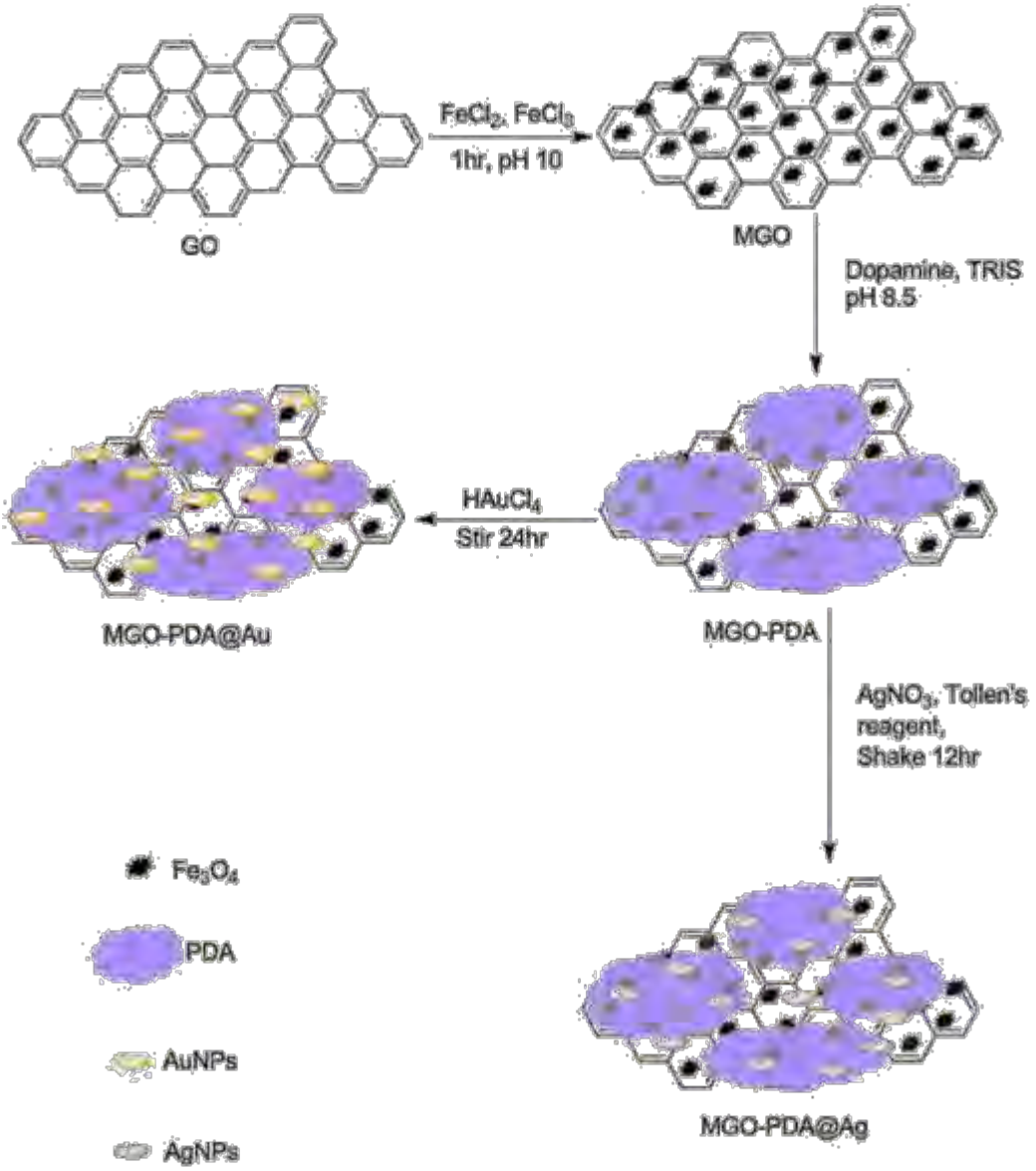

Figure 4.1 Schematic illustration of immobilization of gold and silver nanoparticles onto MGO-PDA nanocomposite. (Tris buffer: tris(hydroxymethyl)-aminomethane buffer).

4.2 Functional Group Characterization by Fourier Transform Infrared Spectroscopy (FTIR)

Fourier Transform Infrared Spectroscopy (FTIR) spectroscopy relies on the fact that most molecules absorb light in the infra-red region of the electromagnetic spectrum. This absorption corresponds specifically to the bond present in the molecule. The frequency range is measured as wave numbers over range 4000-600cm^{-1}. FTIR spectroscopy has characterized, to confirm the functional groups present in synthesized compounds, The Characterization peaks for GO show that the characteristic band of the carboxyl group appears at 3400cm^{-1} (O– H stretching vibration), 1718cm^{-1} (C=O stretching vibration), 1600 cm^{-1} (skeletal vibrations from un-oxidized graphitic domains), 1387 cm^{-1} (O–H deformations in the C–OH groups), 1231cm^{-1} (C–OH stretching vibration) and 1034cm^{-1} (C–O stretching vibration in C–O–C in epoxide)

[12]. The peak at 1718cm^{-1}corresponding to C=O of the carboxyl group on the GO shifts to 1638 cm^{-1}, may be due to the formation of –COO^{-} after coating with Fe3O4.

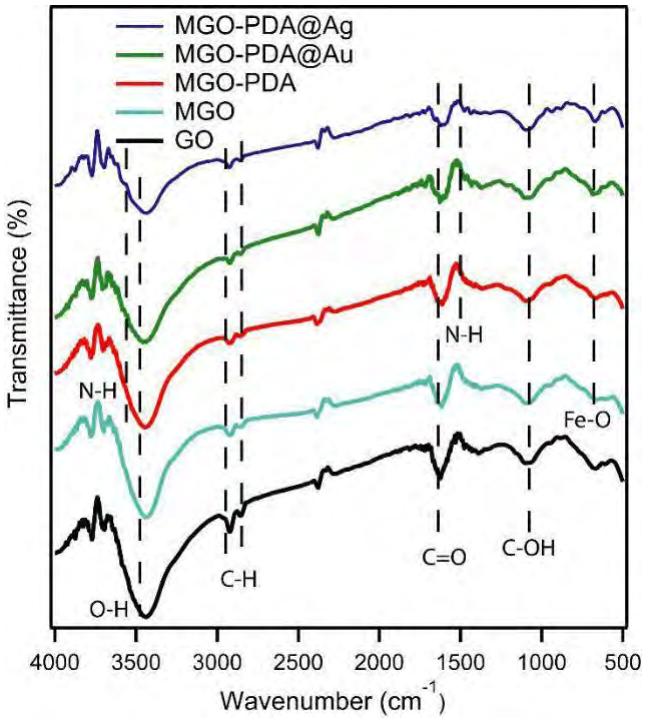

Figure 4.2 FTIR spectra of GO, MGO, MGO-PDA, MGO-PDA@Au and MGO-PDA@Ag.

FTIR spectrum has shown two broad peaks at 1587 and 1084cm^{-1} which correspond to the aromatic C–C stretch and C–O stretch, respectively. The transmittance band around 563cm^{-1} is attributed due to Fe–O [13]. After the deposition of polydopamine, a broad peak at 3406cm^{-1} can be observed, which is contributed to the adsorption of amine groups. The peak at 1600cm^{-1} may be due to the vibration adsorption of C-N group, indicating that the polydopamine coating was successfully obtained [14]. All the peaks of MGO-PDA remain the same in MGO -PDA@Au and MGO-PDA@Ag composites. The corresponding peaks are shown in table 4.1. It shows that the dopamine layer remains same in other two composites. For MGO-PDA@Au and MGO-PDA@Ag nanocomposites the peak position of the functional groups on MGO-PDA still remind and their shapes are similar. This can prove the interaction between AuNPS and AgNPs with MGO -PDA composite by forming an electrostatic attraction.

Table 4.1 Characteristic peak and interpretations correspond to MGO-PDA@Au composite

Functional Group	Wavenumber (cm^{-1})
O–H stretching	3400
C=O stretching	1718
C–C stretching	1587
C–O stretching	1084
Fe–O bending (Fe_3O_4)	563
C–N stretching	1600
N–H bending	3446

4.3 Surface morphology study using Scanning electron microscope (SEM)

The surface morphology was investigated by SEM for MGO, MGO-PDA, MGO-PDA@Au and MGO-PDA@Ag are shown in figure 4. 3 Morphology of MGO (a) flakes prepared by dispersing MGO precipitate in water which is interconnected highly porous structure with pore size ranging from few microns to few tens of microns can be observed in the SEM image of MGO.

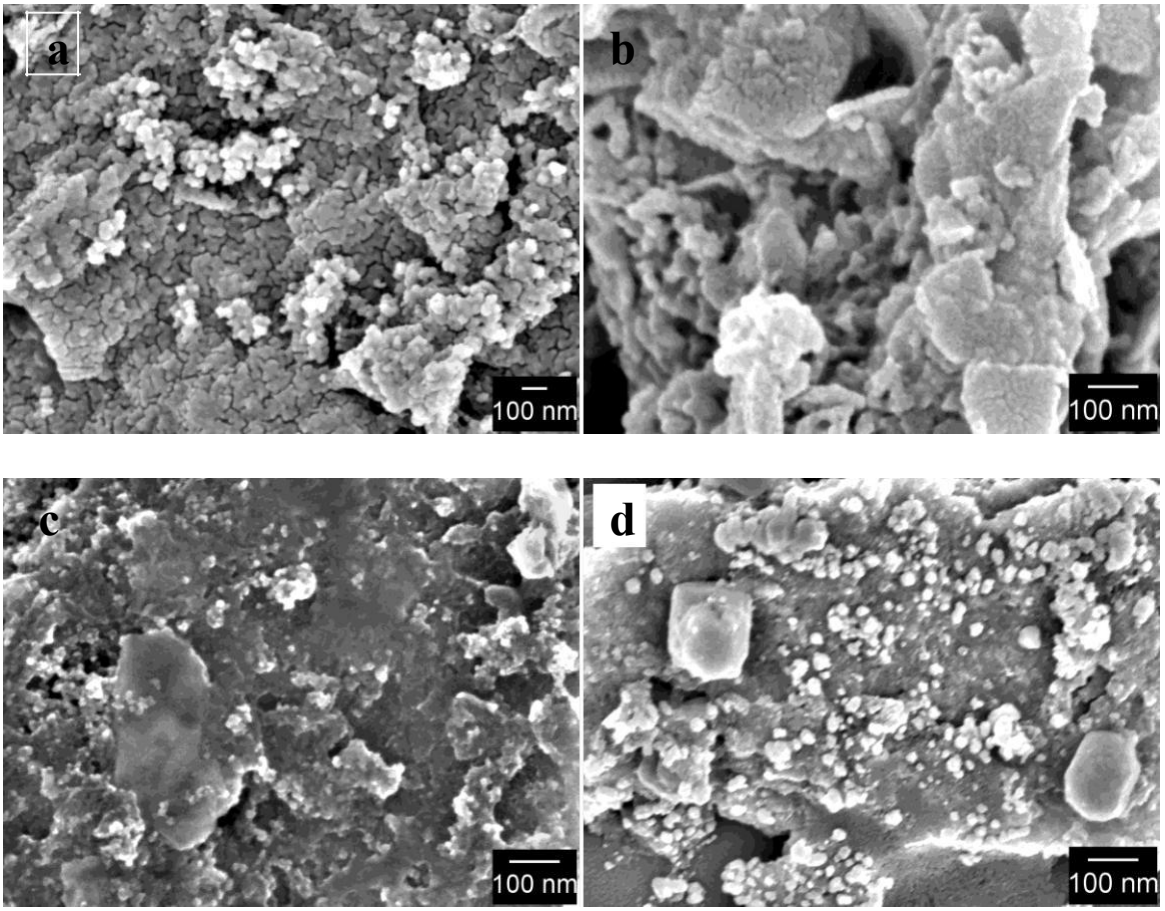

Figure 4.3 SEM images for the surface of MGO (a), MGO-PDA (b), MGO-PDA@Au (c), and MGO-PDA@Ag (d) nanocomposite. Resolution x 100,000**.**

The morphologies of MGO (Figure a) suggest that they have a nearly flake- like shape with characteristic crumpled waves and single- layer nature and show a considerable rough surface

with the magnetite beads on the surface of graphene sheets, which indicate the successful combination of Fe3O4 on the surface of graphene. Uniform size distribution o f NH2–Fe3O4 NPs was found from the SEM (figure b). More interestingly, the NH2–Fe3O4 NPs themselves have mesoporous structures on their surface (figure b). Moreover, the surface of NH2–Fe3O4 NPs was successfully coated with the nanosheets. Figure (c) shows many spherical AuNPs that are deposited on the surface of dopa since the molecular size of Au is smaller than 12 nm; the SEM image has not enough resolution for distinguishing this size. Since PDA acts as a moderate reducing agent and an effective linker [15] [16], AuNPs with controllable density, homogeneous size and uniform distribution. Besides, the PDA film does not damage the characteristic single- layered morphology of graphene. The preservation of original graphene morphology and the attached AuNPs will play an important role in enhancing the analytical performance of the nanocomposite [17]. Figure (d) indicates the coverage of Ag NPs deposition on dopa could be due to the deposition of large amounts of Ag atoms on continuously grown in dopamine layer.

4.3.1 Size Distribution for Au and Ag particles

The average particle size of Au and Ag is measured by software named MIPAR. In that software firstly required SEM image was inserted. The size is plotted against the total number present in percentage. The size range of Au particles is distributed throughout the surface from 5-20nm and the maximum particle size is 8-12nm.

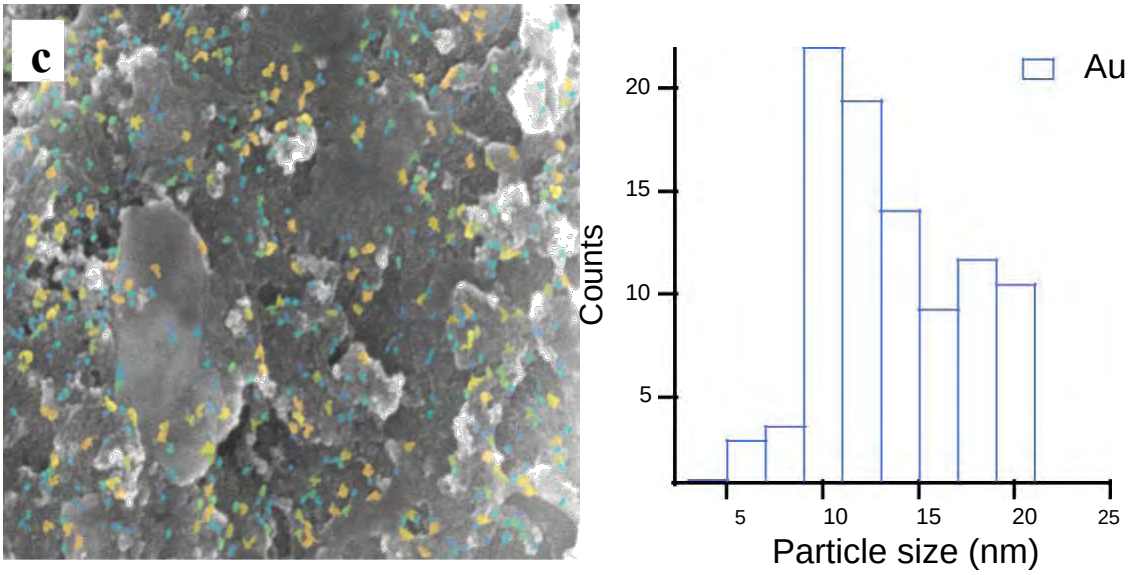

Figure 4.4 The size (equivalent diameter) distribution of Au particles obtained by FESEM.

4.3.2 Size Distribution for Ag particles

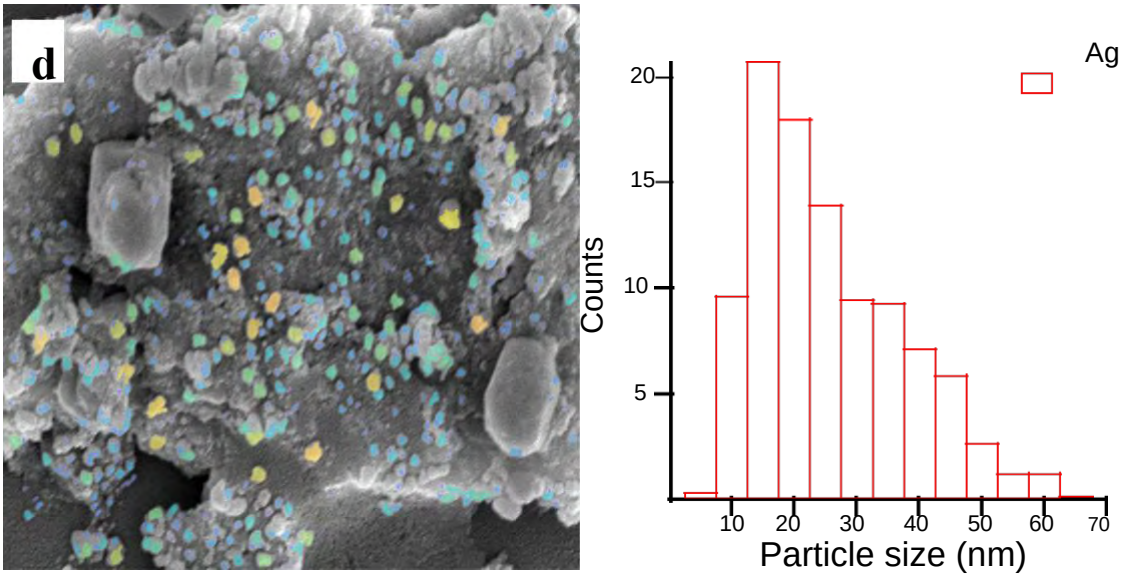

Figure 4.5 The size (equivalent diameter) distribution of Ag particles obtained by SEM. The size range shows Ag particles range from 7-50nm distributed throughout the surface and the maximum particle size placed between 10-25nm.

4.4 Energy Dispersive X-ray Spectral Analysis (EDX)

Elemental analysis of the MGO, MGO-PDA, MGO-PDA@Au and MGO-PDA@Ag nanocomposites has been performed by Energy Dispersive X-ray (EDX) method. In Fig. 4.6(a) the peaks observed at 0.277, 0.525, and 6.398 keV, for K lines of C, O, and Fe respectively. Fig.4.6(b) exhibits that the peaks appear at 0.277, 0.525, 6.398, 0.392 keV for K cell of C, O, Fe and N. Fig. 4.6(c), (d) exhibits that the peaks appear at 0.277, 0.525, 6.398, 0.392, 2,121 and 2,983 keV for K cell of C, O, Fe, N, Au and Ag respectively. So, the EDX data confirms the presence of required elements in synthesized nanocomposites.

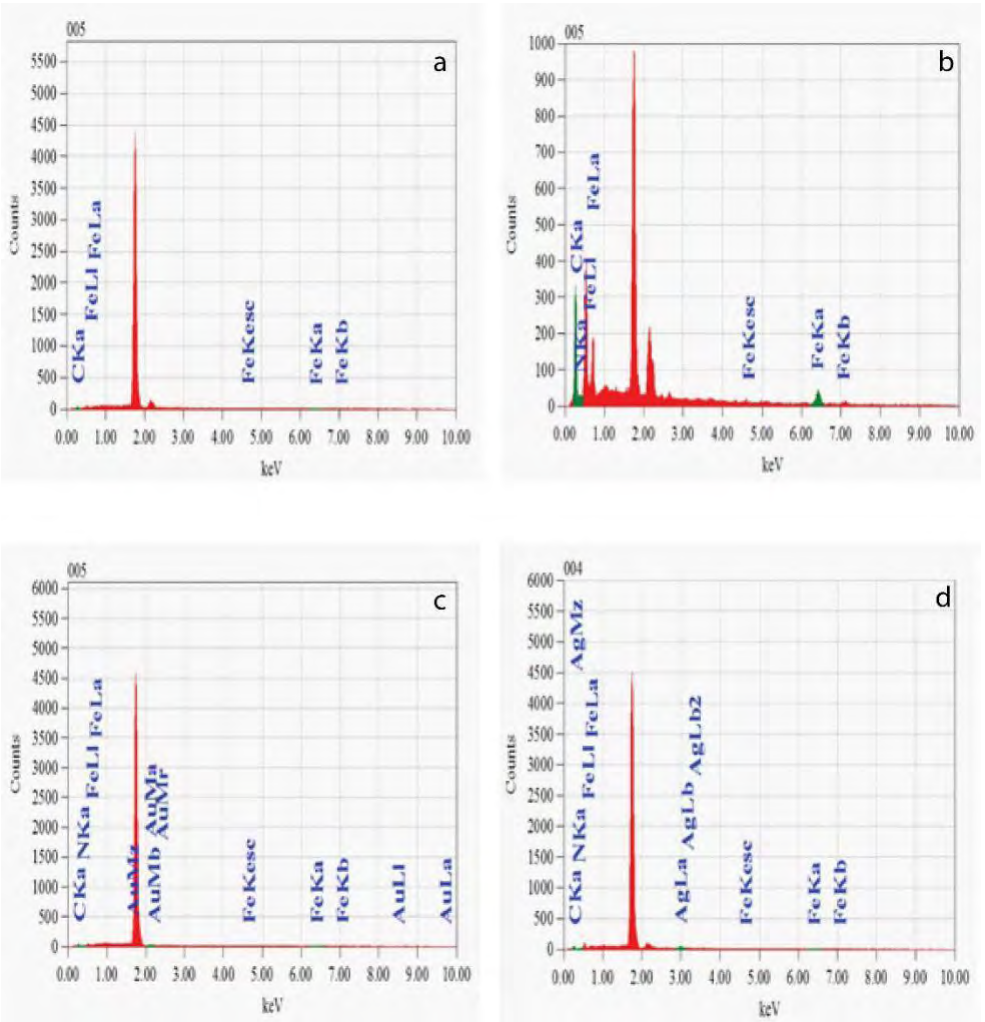

Figure 4.6 EDX spectra of (a) MGO (b) MGO-PDA (c) MGO-PDA@Au, and (d) MGO-PDA@Ag.

4.5 X-ray Diffraction Analysis (XRD)

The crystalline properties, size and phase identification were characterized by X-ray diffraction using a Philips X'pert PRO X-ray diffractometer. The XRD patterns of the synthesized MGO, MGO-PDA@Ag and MGO-PDA@Au composite are shown in Figure 4.7 The peaks (4.7 (a)) at 2θ = 30.1° (220), 35.2° (311), 43.5° (400), 53.9°, 57.2° (511) and 62.8° (440) were consistent with the standard XRD data of Fe3O4 [Joint Committee on Powder Diffraction Standards (JCPDS card No.19-0629)] [3, 18]19].

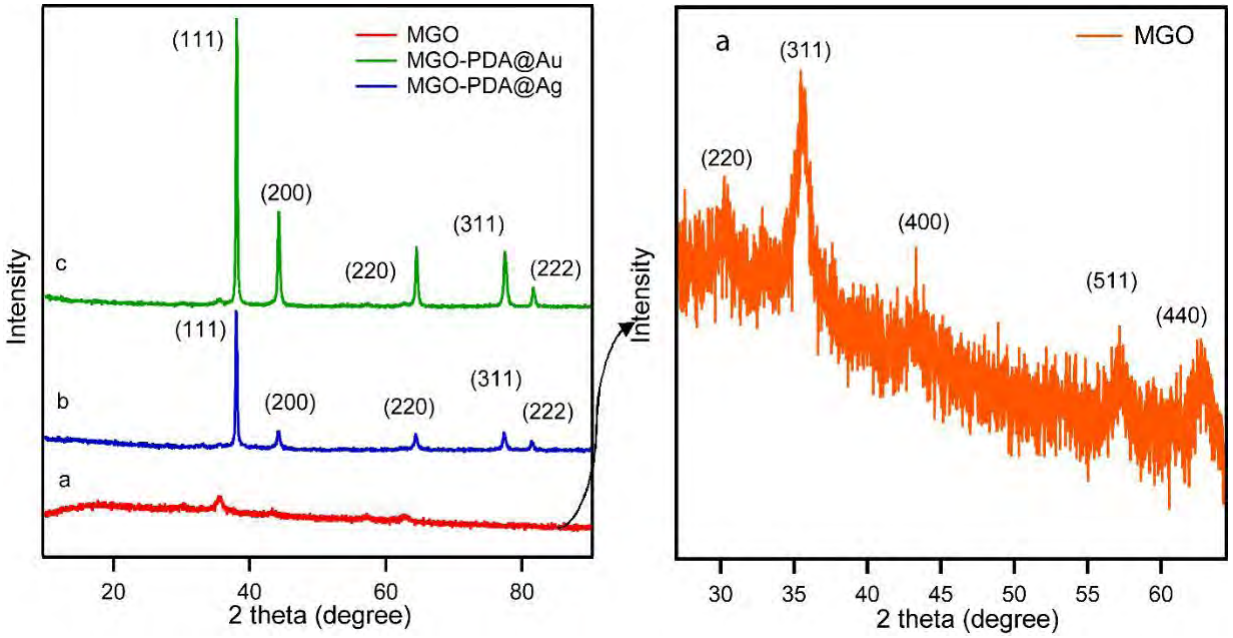

Figure 4.7 XRD spectra of MGO (a), MGO-PDA@Ag (b) and MGO-PDA@Au (c) composite. (a) Zoom in spectra of MGO.

Due to the crystalline nature of silver nanoparticles, intense X-ray diffraction (XRD) peaks were observed corresponding to the (111), (200), (220), (311) and (222) planes for silver at 2θ angles of 38.2°, 47°, 65.27°, 77.6°and 81.7° respectively (Figure 4.7 (b). This was in agreement with the unit cell of the face-centered cubic (fcc) structures (JCPDS file no. 04–0783) [20]. The X-ray diffraction (XRD) pattern of Au nanoparticles is shown in Fig. 4.7 (c) five XRD diffraction peaks at 2θ of 38.0°, 44.4°, 64.5°, 77.2° and 81.6° correspond to the diffraction of the (111), (200), (220), (311), and (222) lattice planes, indicating a face-centered-cube (fcc)

phase (JCPDS 04-0784) of the Au crystal [21]. Since the GO powder does not have a crystal structure, no obvious characteristic peak of GO can be distinguished. A comparison of our XRD spectrum with the standard confirmed that all particles formed in our experiment were in the form of nanocrystals.

4.6 Thermo Gravimetrical Analysis (TGA)

Thermal analysis technique such as thermogravimetric analysis was carried out to measure the thermal stability of MGO-PDA, MGO-PDA@Au and MGO-PDA@Ag nanocomposites at the temperature range 20-800^{0}C. Figures are following the data. The profile for the MGO -PDA showed that it has lower thermal stability than MGO-PDA@Au, because it showed a gradualweight loss with increasing temperature due to the decomposition of the groups containing oxygen which can be attributed due to the evaporation of adsorbed water that weakly adsorbedon the particles surface and a rapid decomposition of the PDA film [22].

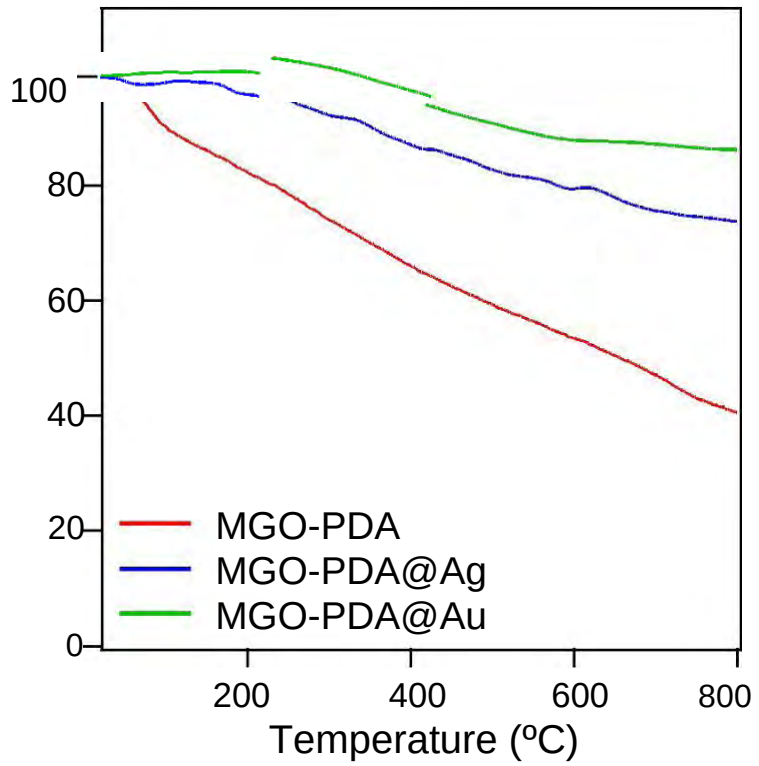

Figure 4.8 Thermogravimetric analysis of MGO-PDA, MGO-PDA@Au and MGO-PDA@Ag.

On the other hand, MGO-PDA@Au and MGO-PDA@Ag have shown the slight degradation at 97 °C for physically absorbed water. Also, there is a steady weight loss until 800 ◦C and around 20% and 30% weight loss are observed respectively. The observed behavior is most likely as a consequence of the surface desorption of bioorganic compounds present in the nanoparticles powder [23, 24]. So, compare to MGO-PDA nanocomposite, we can say that our desired nanocomposites are thermally stable.

4.7 Magnetic Property Analysis

The paramagnetic behavior of MGO and MGO-PDA@Au composite was measured by plotting magnetization curves. The hysteresis loops of MGO and MGO-PDA@Au composite are shown in Fig. 4.9. It can be seen that the magnetic saturation values of these are about 41.9 and 9.2 emu/g respectively. The decrease in magnetic saturation of the MGO -PDA@Au nano-composite in comparison with MGO may be arisen to the increased mass of the polydopamine shell and AuNPs. Despite though the extra weight of MGO-PDA@Au composite exhibits the paramagnetic behavior. The inset photograph shows the magnetic behavior of MGO-PDA@Au composite and it can easily separate from aqueous solution using an external magnet.

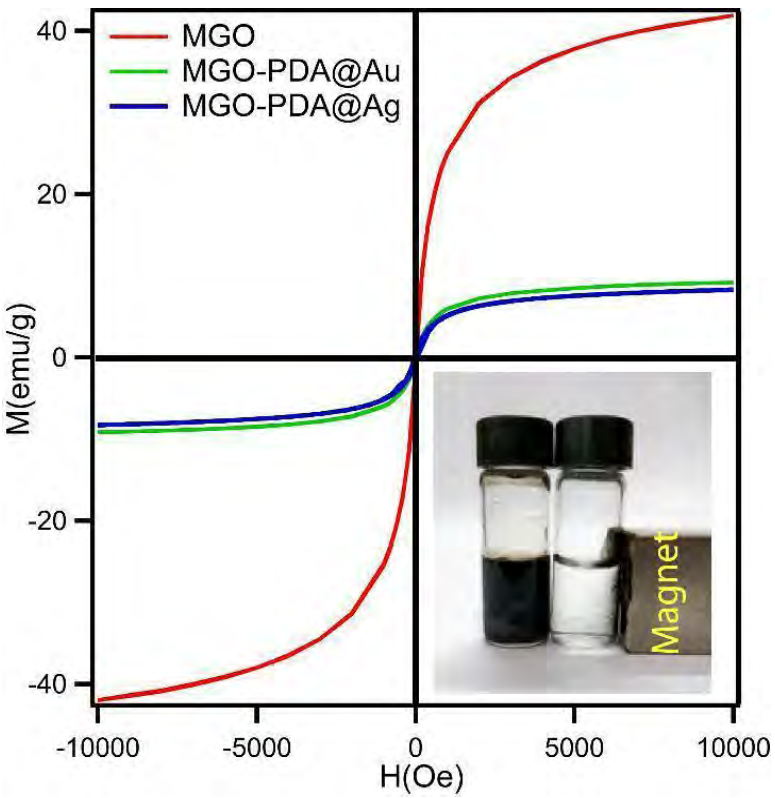

Figure 4.9 Magnetic hysteresis loop of MGO and MGO-PDA@Au nanocomposite. The inset photograph: separation of MGO-PDA@Au composite from aqueous dispersion using a magnet bar.

4.8 Catalytical Reduction of 4-Nitrophenol

4.8.1 Reduction of 4-Nitrophenol by only $NaBH_4$

NaBH4 is a reducing agent. It can reduce 4-NP (yellow color) to 4-aminophenol (4-AP) (pale yellow color). Herein, the reduction of 4-NP by NaBH4 used as a model reaction to investigate the catalytic performance of MGO-PDA@Au composite. This reaction monitored by the color bleaching of 4-NP solution after the addition of NaBH4, as indicated by the gradual decrease in the maximum absorbance value at 400 nm with the time in UV-vis spectra. Fig. 4.10 explore the UV−vis spectra for reduction of 4-NP aqueous solution (0.01 $mmolL^{-1}$) by NaBH4. The spectra show that after 20 min small amount of 4-NP was reduced, it says that the rate of the reaction is very low. Finishing the reaction, it will take several days.

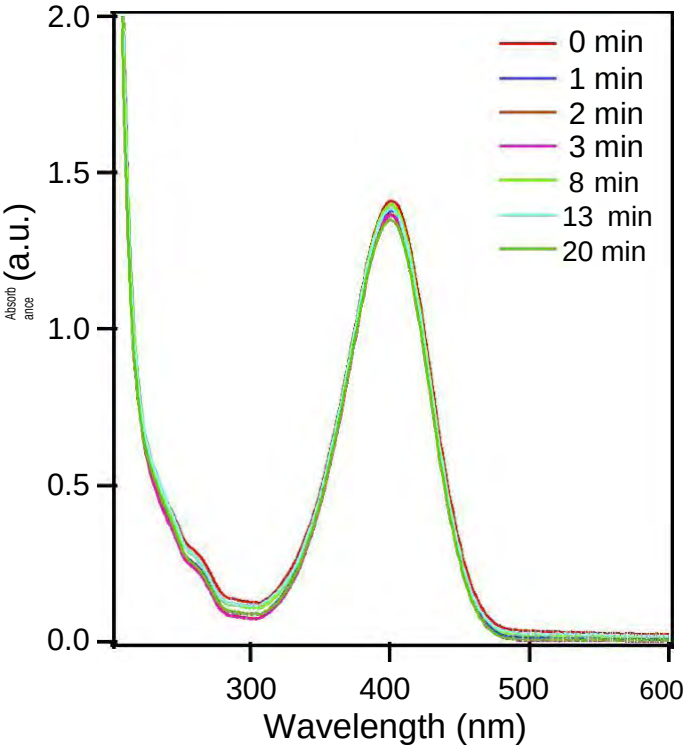

Figure 4.10 The 4-NP reduction reaction monitored by UV-visible spectrophotometry catalysed by only NaBH4.

4.8.2 Reduction of 4-Nitrophenol by MGO-PDA@Au nanocomposite

Catalytic performance of MGO-PDA@Au nanocomposite shown in Fig. 4.11. To evaluate the catalytic activity of MGO-PDA@Au composite, 4-NP solutions were used for the tests. Without the addition of AuNPs as a catalyst, the peak of 4-nitrophenolate anion at 400 nm did not change. Upon the addition of catalyst, it has reduced to 30 while a new peak at 1.2 in 1 min. The new peak at 1.2 exhibited for reduction corresponding to a reaction product 4-NP. The overall reaction was completed near 96.4% in just 7 min.

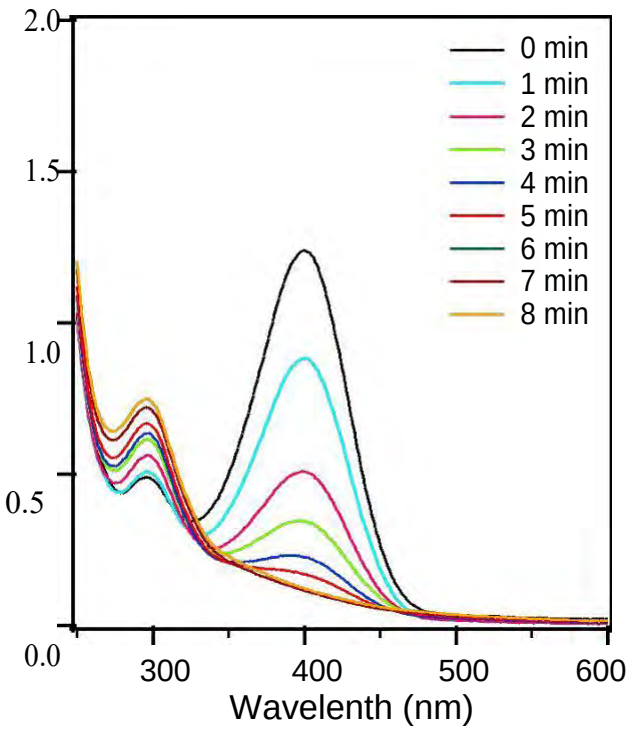

Figure 4.11 The 4-NP reduction reaction monitored by UV-visible spectrophotometry catalysed by MGO-PDA@Au.

4.8.3 Reduction of 4-Nitrophenol by MGO-PDA@Ag nanocomposite

Catalytical reduction of 4-NP shown in Fig. 4.12 where MGO-PDA@Ag was reduced to 1.4 in 1 min. Without the addition of AgNPs as a catalyst, the peak of 4- nitrophenolate anion at 400 nm did not change. Upon the addition of catalyst, it has reduced to 30 while a new peak at 1.4 in 1 min. The new peak at 1.2 exhibited for reduction corresponding to a reaction product 4-NP. The overall reaction was completed near 8 min.

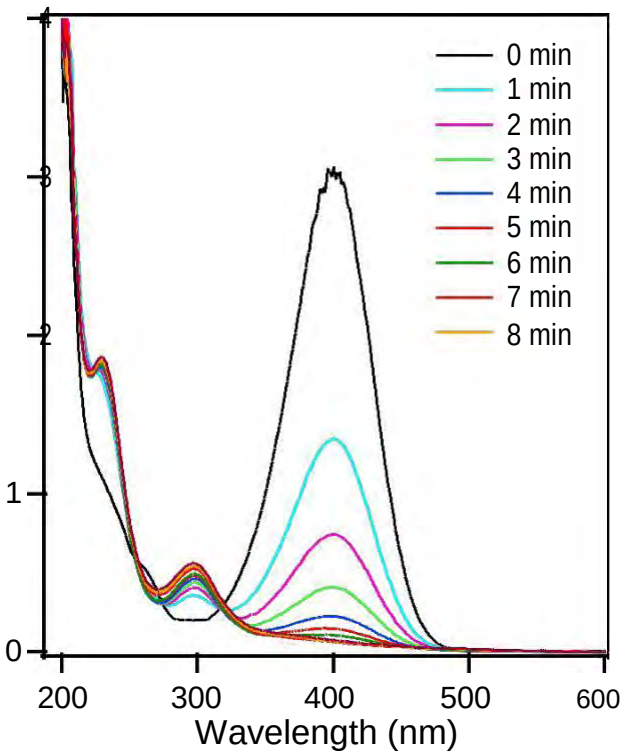

Figure 4.12 The 4-NP reduction reaction monitored by UV-visible spectrophotometry catalysed by MGO-PDA@Ag.

4.9 Catalytical Reduction of Methylene blue

4.9.1 Reduction of methylene blue (MB) by only $NaBH_4$

NaBH4 is a reducing agent. It can reduce MB (color full compound) to leuco MB (colorless compound). Herein, the reduction of MB by NaBH4 is used as a model reaction to investigate the catalytic performance of two noble catalysts. This reaction monitored by the color bleaching of MB solution after the addition of NaBH4, as indicated by the gradual decrease in the maximum absorbance value at 664 nm with the time in UV- vis spectra. Fig. 4.13 explores the UV−vis spectra for reduction of MB aqueous solution (20 ppm) by NaBH4. The spectra show that after 10 min small amount of MB was reduced, it says that the rate of the reaction is very low. Finishing the reaction, it will take several days.

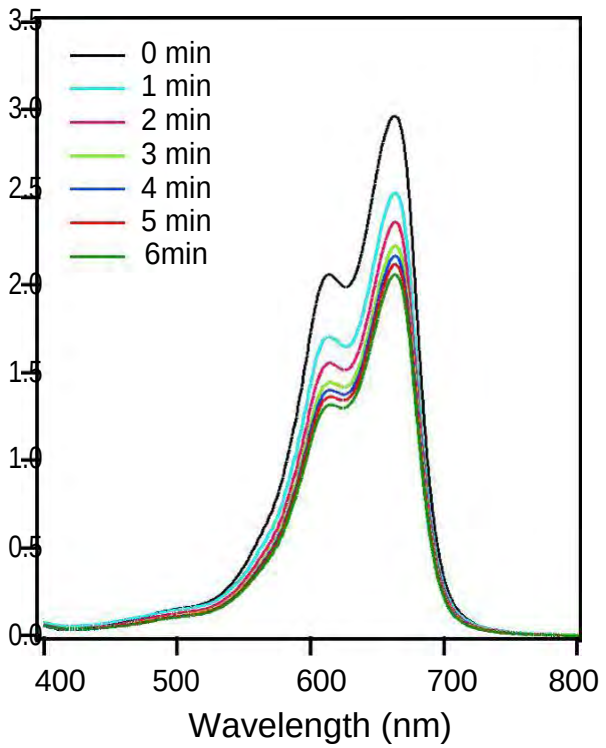

Figure 4.13 The methylene blue reduction reaction monitored by UV-visible spectrophotometry catalyzed by NaBH4.

4.9.2 Reduction of methylene blue (MB) by MGO-PDA@Au nanocomposite.

Catalytic performance of MGO@PDA-Au nanocomposite shown in Fig. 4.14 evaluate that it has shown tremendous performance by reducing maximum MB only just in 0min. MB gives peak at 658 nm and absorbance peak at 3.0 after the addition of catalyst the absorbance goes directly to 0.6 so the total conversion is about 98.9% and to complete the reaction it has just taken 4 min only.

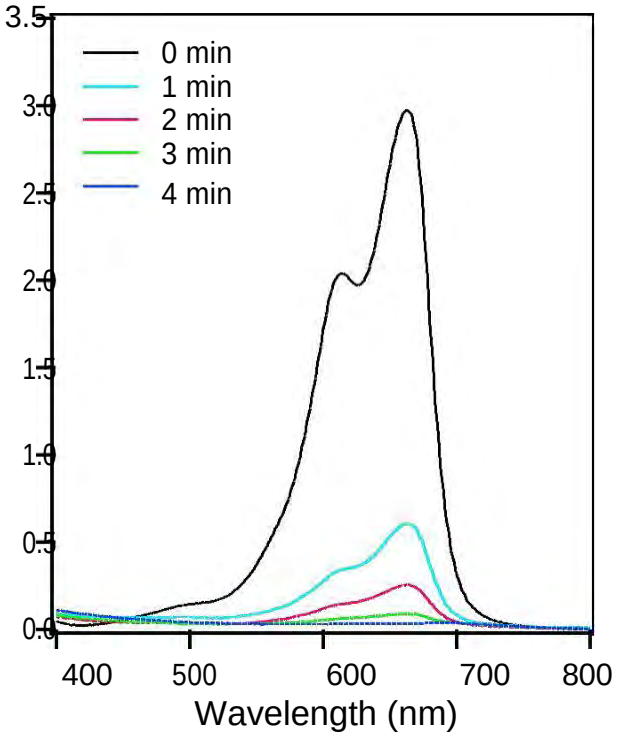

Figure 4.14 The methylene blue reduction reaction monitored by UV-visible spectrophotometry catalysed by MGO-PDA@Au.

4.9.3 Reduction of methylene blue (MB) by MGO-PDA@Ag nanocomposite

Catalytic performance of MGO-PDA@Ag nanocomposite shown in fig. 4.15 To evaluate the catalytic activity of MGO-PDA@Ag initially MB gives a peak at 658 nm and absorbance peak at 3.0 after the addition of catalyst the absorbance goes 1.7 and after the increa sing of time the rate of reduction gradually decreased and took time to finish the reaction.

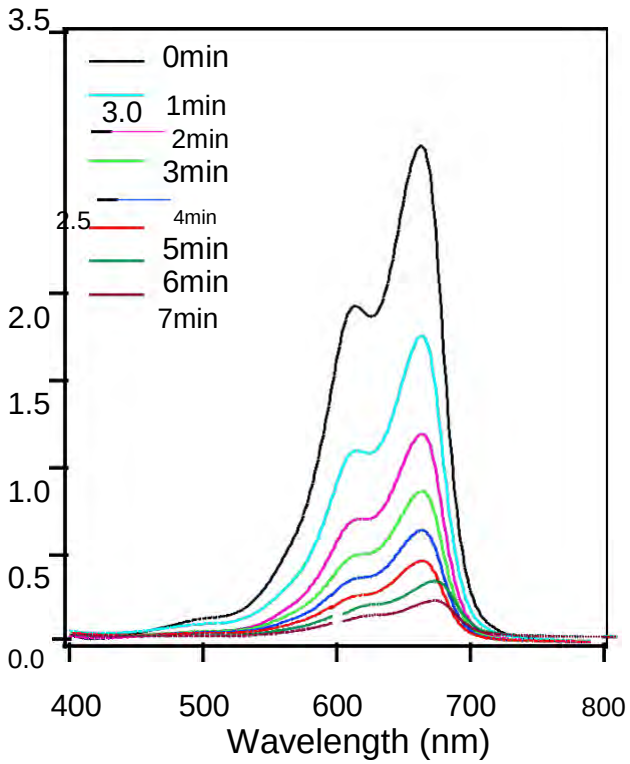

Figure 4.15 The methylene blue reduction reaction monitored by UV-visible spectrophotometry catalyzed by MGO-PDA@Ag.

4.10 Kinetics

The UV-visible data obtained for the catalytic reduction of MB and 4-NP in presence of MGO-PDA@Au and MGO-PDA@Ag nanocomposites were very elusive and therefore it motivated us to study the kinetics further in order to compare their catalytic performances and reaction mechanisms. For the comparison of the catalytic activity of MGO-PDA@Au and MGO-PDA@Ag nanocomposites, the reaction rate constant was obtained directly from the slope of the straight line of ln (C_t /C_0) versus time (t) plot that follows the pseudo-first-order kinetics. The ratios of C_t (the concentration of dye at time t) to C_0 (the initial concentration of dye) can be obtained from the relative intensity ratios of the respective absorbance (A_t /A_0) at 664 nm for MB and 400 nm for 4-NP. From figure 4.16, it can be seen that the reaction rate constant for catalytic reduction of MB in presence of MGO -PDA@Au nanocomposite was found to be 0.995 min^{-1}, whereas, in the presence of MGO-PDA@Ag the rate constant was 0.427 min^{-1}.

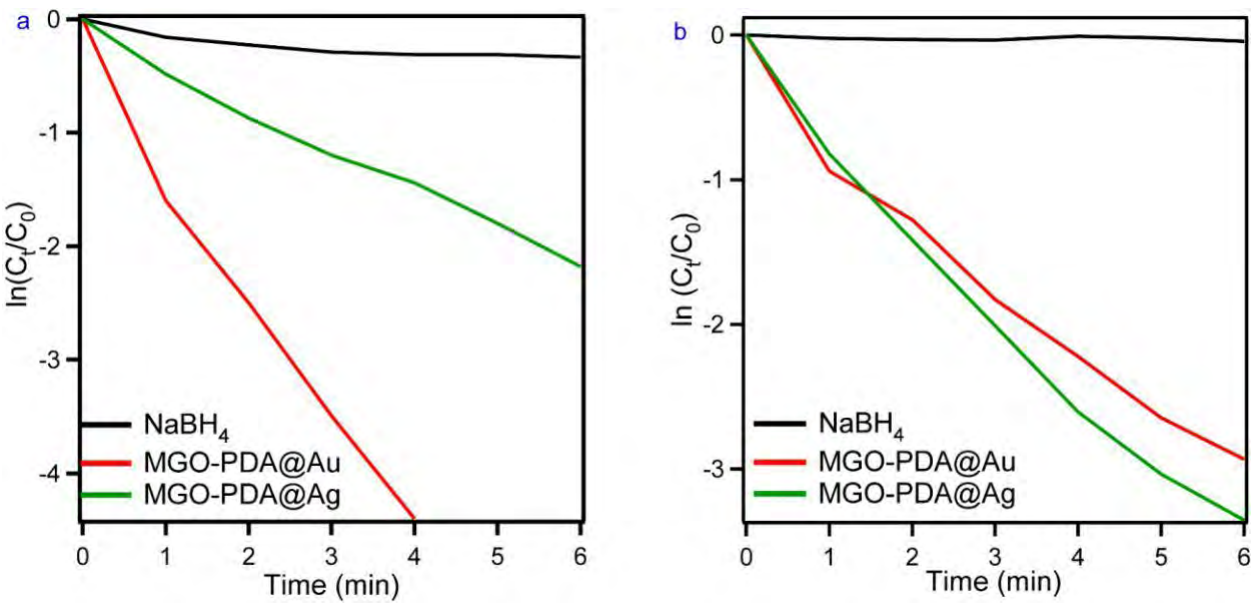

Figure 4.16 Pseudo- first order kinetic plot (ln (C_t /C_0) versus time, t) for the catalytic reduction of (a) MB and (b) 4-NP in presence of MGO-PDA@Au and MGO-PDA@Ag nanocatalysts.

4.11 Recyclability Test

As noble metals which are used as a catalyst sometimes go through staining by reaction products during catalytic reactions. Due to stain the stability of this catalyst can get hamper so the improvement is must maintain the stability for practical applications. In order to test the catalytic stability of the as-synthesized gold and silver nanocomposites, the catalysts were recycled up to 8 times in the presence of NaBH4. After each cycle, the nanocomposite catalyst was isolated from the solution by applying an external magnetic field and reused after washing with ethanol and water for MB. This phenomenon implies a facile and efficient way to separate and recycle the materials from reaction systems. The recycling process of the nanocomposite takes only 10 min to complete. For instance, the average reduction of MB within the 8 cycles was found to be 92% for Au a nd 90 % for Ag. The fast and efficient regeneration of the as-synthesized catalyst along with greater recyclability could be performed due to the stabilizations of the AuNPs and AgNPs by GO network and polydopamine which also prevent the aggregation and hold the particles very strongly.

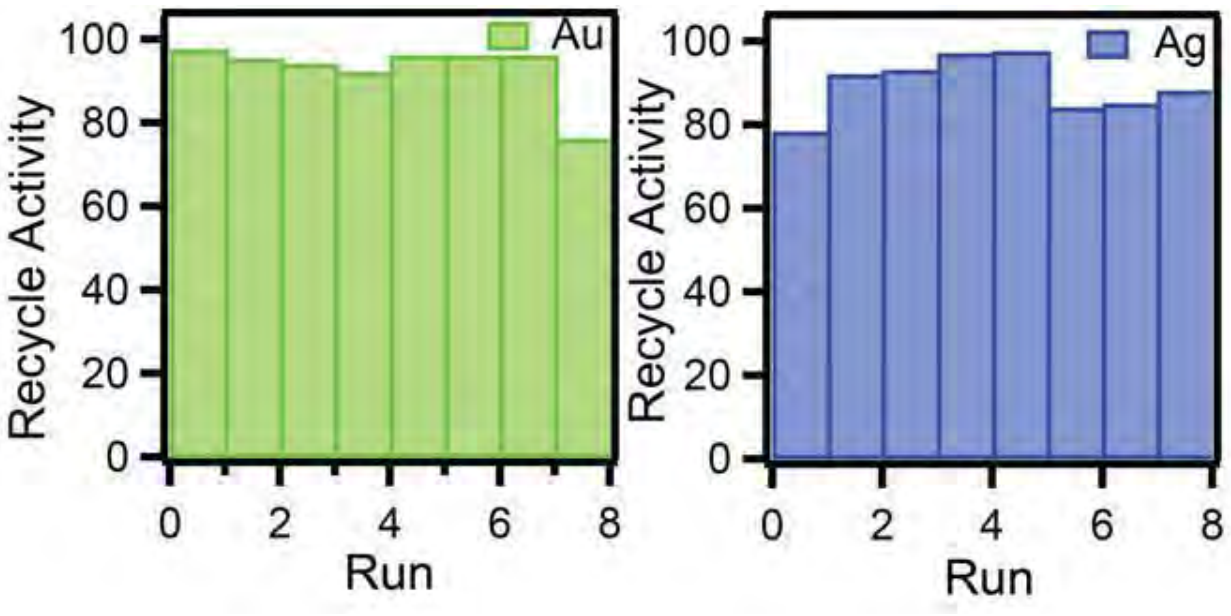

Figure 4.17 Recycling of MGO-PDA@Au and MGO-PDA@Ag for the adsorption of methylene blue.

4.12 Conclusions

In this research, a facile, in situ, and efficient approach was denoted for the synthesis of MGO-PDA@Au nanocomposite. Au- immobilized nanocomposite exhibits excellent catalytic efficacy on the reduction of organic dye 4-NP and MB with NaBH4 as well as fast adsorption rate of MB from aqueous solutions from another noble Ag nanocomposite. The excellent catalytic reduction and adsorption execution can be attributed to the disperse Au NPs onto polydopamine coated with magnetic-GO based nanocomposite as supporting material. The superparamagnetic properties of the MGO-PDA@Au composite enable them to be easily recovered for reuse under an external magnetic field. The versatile mussel- inspired polydopamine and GO flakes as supporting material also allow the further surface functionalization for the development of multifunctional adsorbent materials. Our experiment gives the impression that MGO-PDA@Au nanocatalyst developed to have potential applications over MGO-PDA@Ag nanocatalyst in catalysis and wastewater treatment.

References

[1] A. K. Geim, and K. S. Novoselov, "The rise of graphene," *Nat Mater,* vol. 6, no. 3, pp. 183-91, Mar, (2007).

[2] E. C. H. Sykes, "Graphene goes undercover," *Nature Chemistry,* vol. 1, pp. 175, (2009).

[3] A. A. Balandin, S. Ghosh, W. Bao *et al.*, "Superior Thermal Conductivity of Single-Layer Graphene," *Nano Letters,* vol. 8, pp. 902-907, (2008).

[4] K. I. Bolotin, K. J. Sikes, Z. Jiang *et al.*, "Ultrahigh electron mobility in suspended graphene," *Solid State Communications,* vol. 146, pp. 351-355, (2008).

[5] M. D. Stoller, S. Park, Y. Zhu *et al.*, "Graphene-Based Ultracapacitors," *Nano Letters,* vol. 8, pp. 3498-3502, (2008).

[6] S. Park, and R. S. Ruoff, "Chemical methods for the production of graphenes," *NatureNanotechnology,* vol. 4, pp. 217, (2009).

[7] J. Si, and H. Yang, "Preparation and characterization of bio-compatible Fe3O4@Polydopamine spheres with core/shell nanostructure," *Materials Chemistry andPhysics,* vol. 128, pp. 519-524, (2011).

[8] Y. Tang, F. Huang, W. Zhao *et al.*, "Synthesis of graphene-supported Li4Ti5O12 nanosheets for high rate battery application," *Journal of Materials Chemistry,* vol. 22, pp. 11257-11260, (2012).

[9] A. Alizadeh, G. Abdi, M. M. Khodaei *et al.*, "Graphene oxide/Fe3O4/SO3H nanohybrid:
a new adsorbent for adsorption and reduction of Cr(vi) from aqueous solutions," *RSC Advances,* vol. 7, pp. 14876-14887, (2017).

[10] C.-J. Pan, L.-Q. Pang, F. Gao *et al.*, "Anticoagulation and endothelial cell behaviors of heparin- loaded graphene oxide coating on titanium surface," *Materials Science andEngineering: C,* vol. 63, pp. 333-340, (2016).

[11] Z. Liu, X. Wang, Z. Luo *et al.*, “Removing of Disinfection By-Product Precursors from Surface Water by Using Magnetic Graphene Oxide,” *PloS one,* vol. 10, pp. e0143819-e0143819, (2015).

[12] Y. P. He, S. Q. Wang, C. R. Li *et al.*, “Synthesis and characterization of functionalized silica-coated Fe3O4superparamagnetic nanocrystals for biological applications,” *Journal ofPhysics D: Applied Physics,* vol. 38, pp. 1342-1350, (2005).

[13] X. Yang, X. Zhang, Y. Ma *et al.*, “Superparamagnetic graphene oxide–Fe3O4nanoparticles hybrid for controlled targeted drug carriers,” *Journal of MaterialsChemistry,* vol. 19, pp. 2710-2714, (2009).

[14] F. Tan, M. Liu, and S. Ren, “Preparation of polydopamine-coated graphene oxide/Fe3O4
imprinted nanoparticles for selective removal of fluoroquinolone antibiotics in water,” *Scientific Reports,* vol. 7, pp. 5735, (2017).

[15] X. Xu, Q. Zheng, G. Bai *et al.*, “Polydopamine induced in-situ growth of Au nanoparticles on reduced graphene oxide as an efficient biosensing platform for ultrasensitive detection of bisphenol A,” *Electrochimica Acta,* vol. 242, pp. 56-65, (2017).

[16] S. M. Kang, S.Park, D. Kim *et al.*, “Simultaneous Reduction and Surface Functionalization of Graphene Oxide by Mussel-Inspired Chemistry,” *Advanced FunctionalMaterials,* vol. 21, pp. 108-112, (2011).

[17] H. Liu, P. Xi, G. Xie *et al.*, “Simultaneous Reduction and Surface Functionalization of Graphene Oxide for Hydroxyapatite Mineralization,” *The Journal of Physical Chemistry C,* vol. 116, pp. 3334-3341, (2012).

[18] T. Rusianto, M. Wildan, K. Abraha *et al.*, *Various sizes of the synthesized Fe3O4nanoparticles assisted by mechanical vibrations*, (2015).

[19] M. T. Hossain, M. Hossain, M. H. A. Begum *et al.*, *Magnetite (Fe3O4) nanoparticles forchromium removal*, (2018).

[20] S. Chowdhury, A. Basu, and S. Kundu, “Green synthesis of protein capped silver nanoparticles from phytopathogenic fungus Macrophomina phaseolina (Tassi) Goid with

antimicrobial properties against multidrug-resistant bacteria," *Nanoscale Research Letters,* vol.
9, pp. 365, (2014).

[21] J. Song, L. Xu, R. Xing *et al.*, "Synthesis of Au/Graphene Oxide Composites for Selective and Sensitive Electrochemical Detection of Ascorbic Acid," *Scientific Reports,* vol. 4, pp. 7515, (2014).

[22] J. Shen, Y. Hu, M. Shi *et al.*, "One Step Synthesis of Graphene Oxide−Magnetic Nanoparticle Composite," *The Journal of Physical Chemistry C,* vol. 114, pp. 1498-1503, (2010).

[23] J. Kasthuri, S. Veerapandian, and N. Rajendiran, "Biological synthesis of silver and gold nanoparticles using apiin as reducing agent," *Colloids and Surfaces B: Biointerfaces,* vol. 68, pp. 55-60, (2009).

[24] J. Y. Cheon, and W. H. Park, "Green Synthesis of Silver Nanoparticles Stabilized with
Mussel-Inspired Protein and Colorimetric Sensing of Lead(II) and Copper(II) Ions," *International Journal of Molecular Sciences,* vol. 17, pp. 2006, (2016).